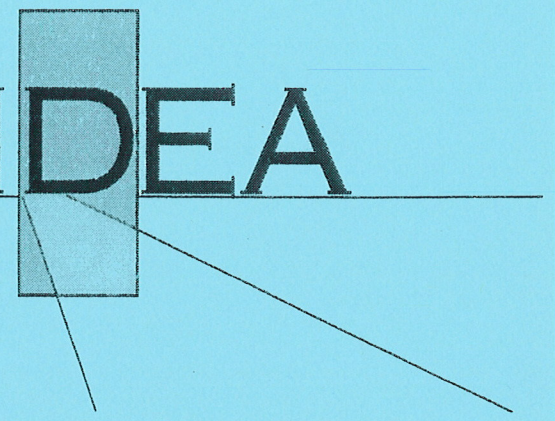

Innovations Deserving
Exploratory Analysis Programs

Highway IDEA Program

Non-Destructive Evaluation Method for Determination of Internal Grout Conditions inside Bridge Post-Tensioning Ducts using Rolling Stress Waves for Continuous Scanning

Final Report for Highway IDEA Project 102

Prepared by:
Yajai Tinkey and Larry D. Olson, Olson Engineering, Inc., Wheat Ridge, CO

December 2006

TRANSPORTATION RESEARCH BOARD
OF THE NATIONAL ACADEMIES

INNOVATIONS DESERVING EXPLORATORY ANALYSIS (IDEA) PROGRAMS
MANAGED BY THE TRANSPORTATION RESEARCH BOARD (TRB)

This NCHRP-IDEA investigation was completed as part of the National Cooperative Highway Research Program (NCHRP). The NCHRP-IDEA program is one of the four IDEA programs managed by the Transportation Research Board (TRB) to foster innovations in highway and intermodal surface transportation systems. The other three IDEA program areas are Transit-IDEA, which focuses on products and results for transit practice, in support of the Transit Cooperative Research Program (TCRP), Safety-IDEA, which focuses on motor carrier safety practice, in support of the Federal Motor Carrier Safety Administration and Federal Railroad Administration, and High Speed Rail-IDEA (HSR), which focuses on products and results for high speed rail practice, in support of the Federal Railroad Administration. The four IDEA program areas are integrated to promote the development and testing of nontraditional and innovative concepts, methods, and technologies for surface transportation systems.

For information on the IDEA Program contact IDEA Program, Transportation Research Board, 500 5th Street, N.W., Washington, D.C. 20001 (phone: 202/334-1461, fax: 202/334-3471, http://www.nationalacademies.org/trb/idea)

Non-destructive Evaluation Method for Determination of Internal Grout Conditions inside Bridge Post-tensioning Ducts using Rolling Stress Waves for Continuous Scanning

IDEA Program Final Report

for the period *04/04* through *06/06*

Contract Number 102

Prepared for the IDEA Program

Transportation Research Board

National Research Council

Yajai Tinkey, Ph.D.

Larry D. Olson, P.E.

Olson Engineering, Inc.

December 11, 2006

ACKNOWLEDGEMENTS

Several groups and individuals contributed to the success of this project, to whom the authors are extremely grateful. In particular, Mr. Jim Fabinski of Encon Bridge Company of Denver, Colorado deserves recognition for donating a full-scale pre-cast bridge girder for use in this research project. We very much appreciate the efforts of Restruction Corporation of Sedalia, Colorado in regards to the grouting of the bridge girder ducts. Our sincere gratitude goes toward Dr. Herbert Wiggenhauser of BAM Laboratory in Berlin, Germany for sharing a mock-up slab for Impact Echo testing with our research team. The IDEA project manager, Dr. Inam Jawed, must be especially thanked for being always available for guidance and providing opportunities for disseminating research information. In addition, the authors would like to express their deep appreciates to Mr. Raul Bedon of Dywidag Systems International, Mr. Randy Cox of the Texas Department of Transportation, Mr. Larry Sessions of the Florida Department of Transportation and Mr. Mohammad Sheikhizadeh of the Washington Department of Transportation for volunteering their valuable advice in design and construction of grout defects. Finally, the financial support from the NCHRP-IDEA program is greatly appreciated.

TABLE OF CONTENTS

1.0 EXECUTIVE SUMMARY

The objective of the research project is to develop reliable nondestructive near-continuous scanning methods for condition assessment of the internal grout conditions inside bridge ducts. Different sizes of ducts were included in this study as well as varying sizes of void defects. In addition, detailed sensitivity studies of nondestructive grout defect detection with Impact Echo Scanning of 8-four inch diameter ducts with constructed defects were the main research focus.

Two specimens were used in this research project. The first specimen used for this study was a large mock-up slab located at the BAM facility in Berlin, Germany. The size of the slab is 32.8 x 13.1 ft (10 x 4 m) with a nominal thickness of 11.8 inches (30 cm). The mock-up slab was constructed in 2002 for the purpose of blind studies of grout defect detection with different non-intrusive methods. Half of the mock-up slab includes ducts with the diameters ranging from 1.57 to 4.72 inches (40 to120 mm). Concrete cover depths above the ducts varied from 2.75 to 7.5 inches (70 to 190 mm). The other half of the slab includes different types of internal voids and other simulated defects.

The research also included the first attempt to develop a complete stress wave scanner by adding another rolling displacement transducer 8 inches (20 cm) in a line from the first rolling transducer. This additional rolling transducer allows Spectral Analysis of Surface Wave tests for concrete quality/condition/velocity to be performed at the same time as thickness/flaw detection tests are conducted with the Impact Echo Scanning test. Improvements in software were implemented to support simultaneous analysis of data from both tests.

A compete stress wave scanner was used to perform SASW and IE tests on the BAM mock-up slab. The tests were performed in a line fashion parallel to the direction of the ducts every 5 cm. A total of 200 test lines were performed to cover the whole slab area. Table I summarizes the grout defect size that can be detected in ducts of different diameters and concrete covers. Reviews of Table I show that half size and full size voids can be detected with the IE tests in 4.72 and 3.94 inches in diameter. Only full size voids can be detected inside ducts with a diameter of 3.15 inches. However, once the concrete cover is 5.5 inches and higher, the IE results become intermittent and unreliable. In summary, it is easier to detect grout defect in ducts with bigger diameters. In addition, the deeper the duct is inside the concrete, the harder it is to detect grout defects with the IE tests.

Table 1 – Impact Echo Scanning Duct Void Sensitivity Study Results from the BAM Mock-up Slab

Duct Diameter (inches)	Cover (inches)	Half Size Void Detected	Full Size Void Detected
4.72	2.76	Yes	Yes
3.94	3.15	Yes	Yes
3.15	3.94	No	Yes
3.15	5.5	No	No
3.15	6.7	No	Yes/No
2.36	3.94	No	Yes
1.57	4.33	No	Yes
1.57	6.7	Yes	Yes
1.57	7.48	No	No
1.57	1.97 - 6.3	No	Yes

Technical problems occurred during the use of the stress wave scanner with variability in contact conditions between the second rolling transducer and the test surface in SASW tests. Consequently, data from the second rolling transducer were intermittent. However, good data from the second rolling transducer were still generally obtained. These data showed an approximate 11% reduction in surface wave velocity at locations associating with grout void.

The second specimen used in this study is a full scale U-Shaped bridge girder. The length of the girder is 100 ft. However, only the first 20 ft was included in this study. There were four empty steel ducts inside each wall of the girder (a total of 8 ducts). The diameter of each duct is 4 inches. Several pieces of Styrofoam were inserted inside the duct. The foam was positioned on the roof of the duct to simulate real world grout defect. The size of the foam used ranged from as small as 16% duct perimeter lost or 6% depth lost to 84% perimeter lost or 94% depth lost (void). The use of 3D surface plotting of the IE thickness results was helpful with interpretation and visualization of grout defects. A grout

defect as small as 20% perimeter lost or 11% depth lost in 4" duct was detected by the IE tests with the interpretation using 3D surface plotting. The 3-D visualization with a color scale of the thickness change from normal (fully grouted duct) to thicker (partial to full void) proved to be an important tool for imaging sound grout versus partial to full void conditions for both the BAM and U-Shaped girder test specimens. The 3-D color scales proved to indicate very good precision at indicating the size of the internal voids as reflected by increasing thickness echo depths with increasing void size as reported herein. Such visualization of Impact Echo Scanning results allows for much greater sensitivity and economical, near-continuous testing of real-world bridge ducts.

The last part of the research project focussed on the use of the Ultrasonic Pulse Echo test. A commercial unit (Low Frequency Flaw Detector – A1220) was used to perform the UPE test. The UPE test was able to detect the thickness of the wall where no ducts exist inside correctly. However, the UPE test was unable to detect beyond the duct once the ducts are present. This is potentially because of debonding problem between grout and the metal ducts which had occurred by the time of the UPE testing of the comparatively old ducts. Thus, no information was gained from UPE tests on the internal grout conditions in terms of the degree of the voiding in the duct.

2.0 PROBLEM STATEMENT

Post-tensioned systems have been widely used for bridge transportation systems since late 1950s. However if a good quality control plan is not implemented during construction, there is the potential problem during construction that the duct may not be fully grouted. This results in voids in some areas or inefficient protection for prestressing steel. Over the long-term, water can enter the tendon ducts in the void areas resulting in corrosion of the tendon. The collapse of the Brickton Meadows Footbridge in Hampshire in 1967 is the first serious case of corrosion of tendons leading to major catastrophe (1). In 1985, the collapse of a precast segmental, post-tensioned bridge in Wales (Ynys-y-Gwas Bridge) was attributed to corrosion of the internal prestressing tendons at mortar joints between segments (1 and 2). Corrosion-related failures of post-tensioning tendons have been found in several major segmental bridges such as the Niles Channel Bridge near Key West, FL in 1999 and Midway Bridge near Destin, FL in 2000 (3). In addition to actual failures, corrosion damage was found in many post-tensioned bridge ducts in bridges still in use in Florida and East Coast areas (4).

In post-tensioned structures, quantifying the incidence of corrosion is further complicated by limitations in techniques for detecting corrosion. Condition surveys of post-tensioned structures are often limited to visual inspections for signs of cracking, spalling and rust stain. This limited technique may overlook corrosion activity. Corrosion damage in post-tensioned elements has been found in situation where no exterior indications of distress were apparent (4). As a matter of fact, the Ynys-y-Gwas Bridge in Wales had been inspected 6 months prior to the collapse, and no apparent signs of distress were observed (2). Examples such as this one lead some to fear that inspection based on limited exploratory or visual inspections may be unconservative and may produce a false sense of security. Therefore, it is important to develop a reliable method to inspect the quality of grout fill inside the ducts non-destructively after the grouting process is complete and for inspection of older bridges.

3.0 CONCEPT AND INNOVATION

This research project proposed to develop an effective and reliable non-destructive evaluation method to determine the internal grout condition inside bridge ducts using scanning stress wave techniques. The stress wave techniques of interest include Impact Echo (IE), Spectral Analysis of Surface Waves (SASW) and Ultrasonic Pulse Echo (UPE) tests. The scanning technology is very innovative and was developed by Olson Engineering. The original Impact Echo Scanner was first developed and patented in the mid 1990's by Olson Engineering, Inc. and then used as part of a prestressed concrete cylinder pipe research project for the US Bureau of Reclamation (5). This scanning device has a rolling transducer assembly incorporating six transducers attached underneath the test head. When the test head is rolled across the testing surface, an opto-coupler on the central wheel keeps track of the distance. This unit is calibrated to send an impact at intervals of 1 inch. If the concrete surface is smooth, a coupling agent between a rolling transducer and test specimen is not required. However, if the concrete surface is rough, water can be used as a coupling material. Photographs of the Impact Echo Scanner (IES) and the traditional Impact Echo (IE) unit are shown in Fig. 1.

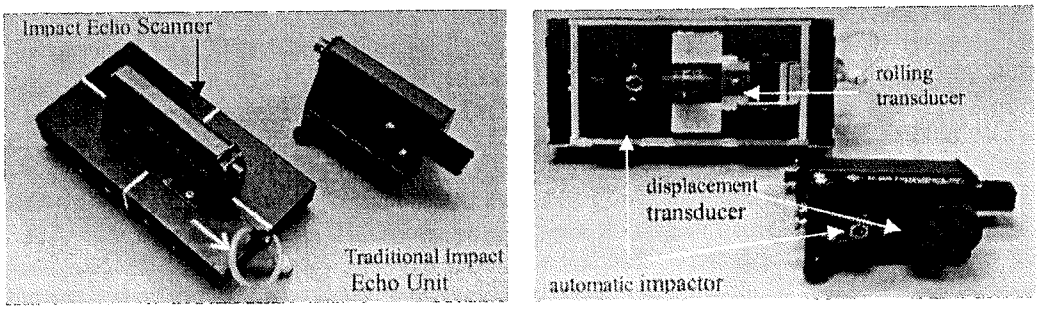

Fig. 1 – Impact Echo Scanning Unit and Traditional Impact Echo Unit

To add the ability to measure surface wave energy to the current practice of Impact Echo Scanning, a new unit was built with one additional rolling transducer 8 inches (20 cm) away and inline with the existing roller transducer as shown in Figure 2. This extra rolling transducer allows for additional Spectral Analysis of Surface Waves (SASW) testing at the same time as Impact Echo testing of the structure. The results from the SASW tests provide for surface wave velocity profile at the tested location. This information significantly improved the reliability of the current practice using Impact Echo Scanning by allowing for nondestructive prediction of the IE velocity.

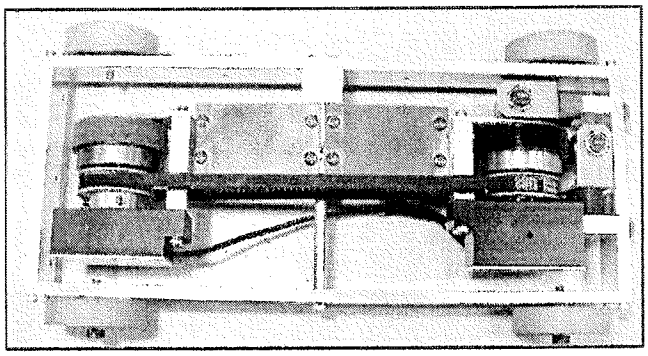

Fig. 2 – A Prototype of Impact Echo Scanning Unit with Additional Rolling Displacement Transducers for Simultaneous Spectral Analysis of Surface Waves and Impact Echo Testing (Open Frame)

Additional studies in the Impact Echo test focused on the sensitivity of the IE test and suitable frequency range for this application using two mock-up specimens. The Ultrasonic Pulse Echo test was also included in this study with a commercial point-by-point test system for evaluation of this technology and for comparison with IES results in terms of grout void detection.

4.0 INVESTIGATION APPROACH

4.1 Introduction

The objective of the research is to develop a reliable technique using various methods non-destructively including Impact Echo (IE), Spectral Analysis of Surface Waves (SASW) and Ultrasonic Pulse Echo (UPE) to evaluate the internal grout condition of post-tensioned bridge ducts. The product(s) from this research is to be used as a tool for inspection of voids inside bridge ducts as soon as the internal grout hardens.

The original Impact Echo Scanner was first developed and patented in the mid-1990's by Olson Engineering, Inc. as part of a research project funded by the US Bureau of Reclamation. The investigation approach for this research project initially started with an evaluation of the current state of the art technology using an existing Impact Echo scanner. The specimen used in this study was a large mock-up concrete slab located at the BAM main campus in Berlin, Germany. The description of the large concrete slab is included in Section 4.2. After learning the limitations of this early version of the IE scanner, improvements in the IES hardware and software were implemented. The improvement in the hardware included adding additional rolling transducer to the scanner unit for Spectral Analysis of Surface Waves testing.

The improvement in the software included data acquisition and analysis functions for the SASW test and an implementation of the three dimensional display of the IE thickness results for grout defect visualization. The hardware and software improvements are detailed in Section 5.0. Another round of IE and SASW tests were repeated on the same mock-up slab at the BAM main campus with the new improved hardware unit and software.

The second stage of the investigation included design and construction of voids inside bridge ducts. A full scale pre-cast bridge girder was donated to the research for use in the grout defect sensitivity studies. There were four empty metal ducts (4 inches in diameter) inside each wall. Modified Styrofoam rods (4 inches in diameter) were inserted into the ducts before grouting to form internal voids with sizes ranging from small to almost full diameter voids for sensitivity studies of IES testing to detect grout defects. The last stage of the investigation was focused on the implementation of Impact Echo Scanning (IES) and Ultrasonic Pulse Echo (UPE) method on the mock-up girder to determine the smallest flaw size that could be located inside the 4 inch ducts.

4.2 Specimens

Two mock-up specimens were used in the study. The first specimen used in the first stage of the investigation is a mock-up slab located at the BAM facility in Berlin, Germany. The description of the mock-up wall is included in Section 4.2.1. The second specimen is a full scale pre-cast girder with eight steel ducts inside. The description of the mock-up girder is included in Section 4.2.2. Finally, construction of the modified Styrofoam defects for the mock-up girder is described in Section 4.2.3.

4.2.1 Description of Mock-up Slab

A mock-up concrete slab was designed and constructed at the BAM main campus in Berlin, Germany in 2002 (6). The picture of the mock-up slab is shown in Figure 3. The concrete slab covers an area of 32.8 x 13.1 ft^2 (10 x 4 m^2) with a nominal thickness of 11.8 inches (300 mm). The large dimensions of the specimen are necessary to minimize boundary effects on the measured signals and to establish well-defined defects without interference between them.

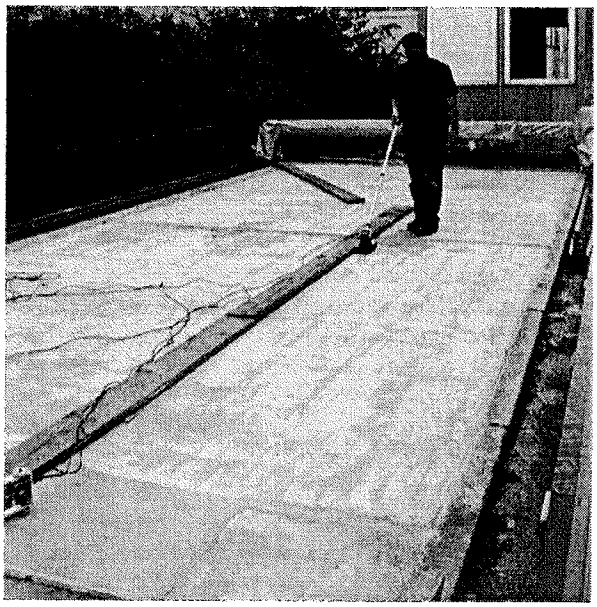

Figure 3 – Impact Echo Scanning on Mock-up Slab at BAM Laboratory (Berlin, Germany)

The concrete slab is partitioned in two sections referring to different testing problems. One section contains tendon ducts with varying diameters and grouting defects and different amounts of post-tension wire strand cables (see Figures 4 and 5). The other section provides areas with varying thickness and voids. Auxiliary elements like thermo-elements, water inlet and reinforcement mats are also embedded in the slab. In addition, 32.8 ft (10 m) long ducts with 11.8 inch (300 mm) spacing are embedded below the bottom of the slab in the subsurface to allow future X-ray radiography for detailed reference testing.

The concrete slab section with metal tendon ducts has dimensions of 13.1 x 16.4 ft (4 x 5 m) and contains eleven tendon ducts with well-defined grouting defects (Figure 4). The metal ducts were chosen and positioned to represent typical testing situations as they are encountered in structures. Because of the difficult testing problem, test situations were created without introducing crossing ducts.

Tendon ducts with the following properties were built-in:

- Diameter: 1.57, 3.15, 3.94, and 4.72 inches (40, 80, 100, and 120 mm)
- Concrete Cover: 2.75, 3.15, 3.94, 4.33, 4.52, 5.5, 6.7, 7.5 inches (70, 80, 100, 110, 115, 140, 170, 190 mm) and one sloped duct 1.96 – 6.3 inches (50 – 160 mm) deep
- Size and location of grouting defects: the size of each of the grouting defects is at least 7.9 inches (200 mm) in length and represents either a fully ungrouted section (void) or a half-filled duct. (The exact position of the defects is not revealed to the public herein in order for others to be able to perform future blind tests.)
- Varying numbers and position of wire strand cables (individual diameters of 0.6 inch) in the tendon ducts.

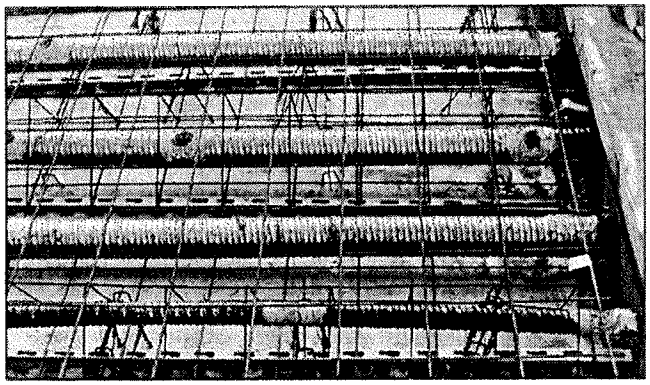

Figure 4 – Different Diameter of Ducts inside the Mock-up Slab

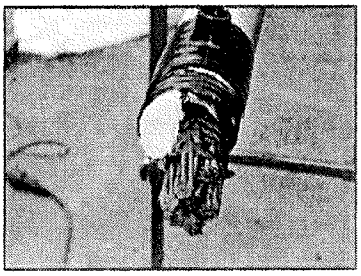

Figure 5 – Example Grout Void

4.2.2 Description of Full Scale Pre-cast Bridge Girder

A full scale pre-cast bridge girder (U-Shaped) was donated to the research team by the Encon Bridge Company for use in grout defect sensitivity studies as part of this research project. The length of the girder is 100 ft (30.48 m) with a typical wall thickness of 10 in (25.4 cm). There were four empty metal ducts (4 inches or 101mm in diameter) inside each wall Figure 6 shows a sketch of the end cross-section. The west end of the girder (20 ft or 6.1 m long) as shown in Figure 7 was selected for this study. Stepped and tapered Styrofoam rods (4 inches or 101 mm in diameter) were inserted into the ducts before grouting to form internal voids with sizes ranging from small to full diameter voids.

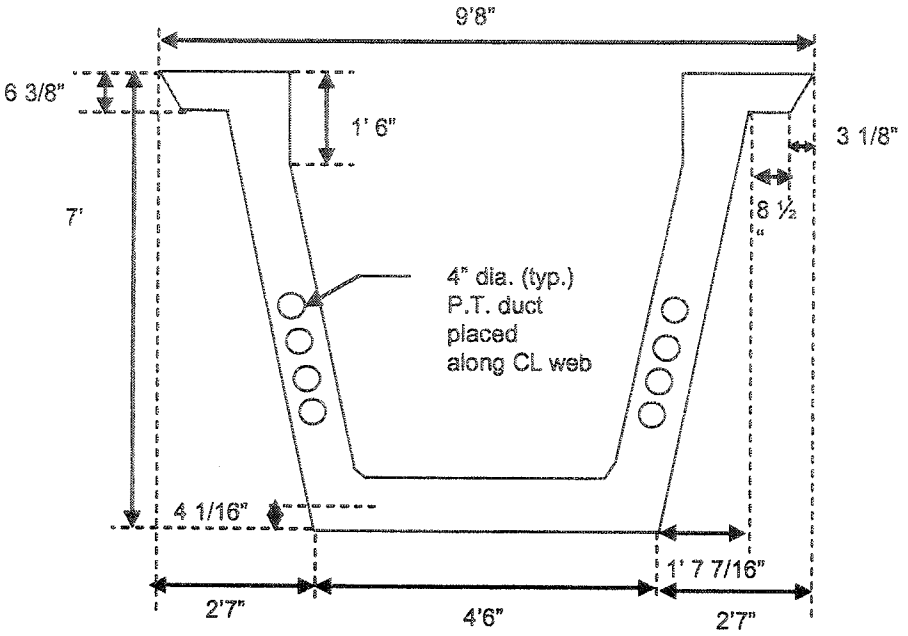

Figure 6 – Cross Section of the End of the U-shaped Girder (not to scale)

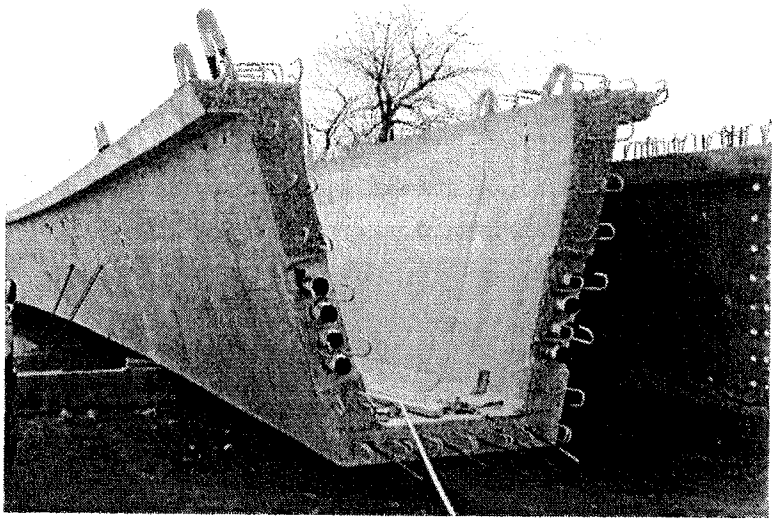

Figure 7 – U-Shaped Bridge Girder (West End)

4.2.3 Design and Construction of Internal Grout Voids

Modified Styrofoam rods (4 inches or 10.16 cm in diameter) were inserted into the ducts before grouting to form internal voids with sizes ranging from small to almost full diameter voids. Figure 8 shows a Styrofoam rod being inserted into the top duct of the north wall. A wire (1/8 inch or 3 mm in diameter) was bent to form a leg for the Styrofoam rod (see Figure 9) so that the foam would be positioned on the roof of the duct, which simulates the real world grout defects formed by air and water voids. Smaller defects were glued directly to the roof of the duct since they were too thin for the wire leg. Figure 10 shows a front view of a Styrofoam defect inside a duct. The defect sizes are presented in Table 1 in terms of their circumferential perimeter and depth lost. The defect designs are shown in Figure 11 for all four ducts in the South web wall and in Figure 12 for the North web wall. The percentage of circumferential perimeter and diameter depth lost due to the defects are shown in the underlined numbers placed directly above the defects in Figures 11 and 12.

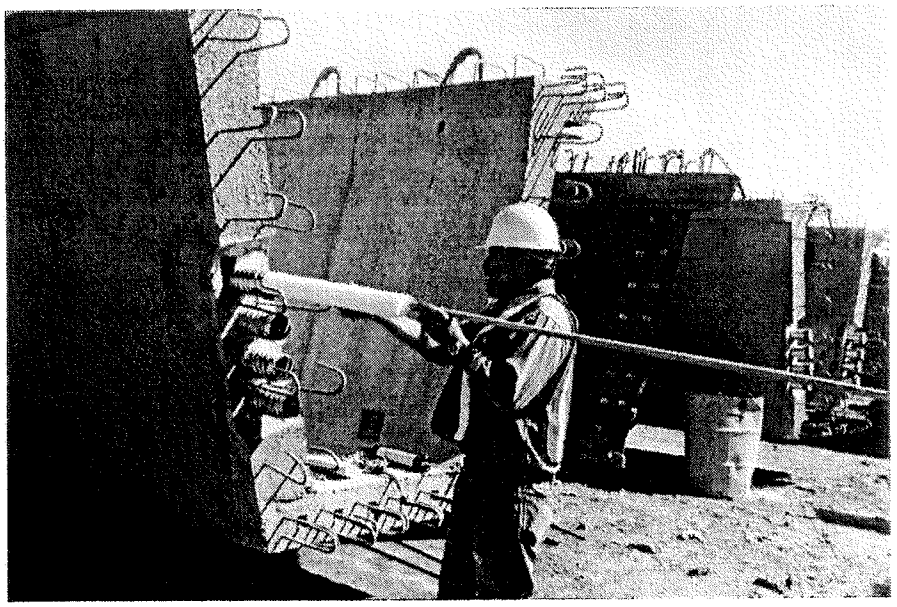

Figure 8 – Styrofoam rods being inserted into the duct

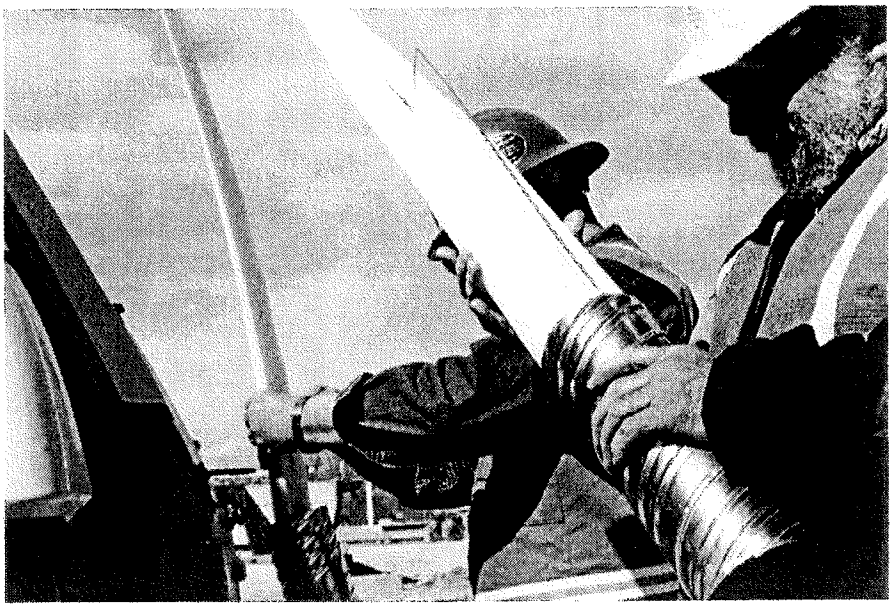

Figure 9 – Wire used to support the Styrofoam rod

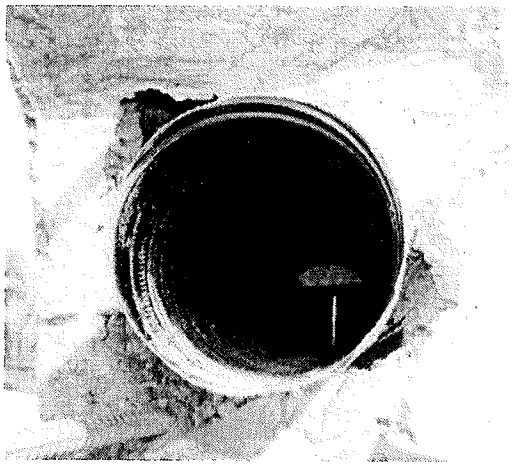

Figure 10 - View of Styrofoam defect inside a duct

Table 1 – Styrofoam Defect Sizes

Defect ID	Circumferential Lost (cm, in)	Duct Depth Lost (cm, in)	Percentage Lost in Circumferential Perimeter (%)	Percentage Lost in Depth (%)
1	5.08, 2	0.635, 0.25	16	6
2	7.72, 3	1.36, 0.535	24	13
3	10.16, 4	2.34, 0.92	32	23
4	12.7, 5	3.48, 1.37	40	34
5	15.95, 6.28	5.08, 2	50	50
6	19.23, 7.57	6.68, 2.63	60	66
7	21.77, 8.57	7.82, 3.08	68	77
8	24.31, 9.57	8.79, 3.46	76	87
9	26.85, 10.57	9.52, 3.75	84	94

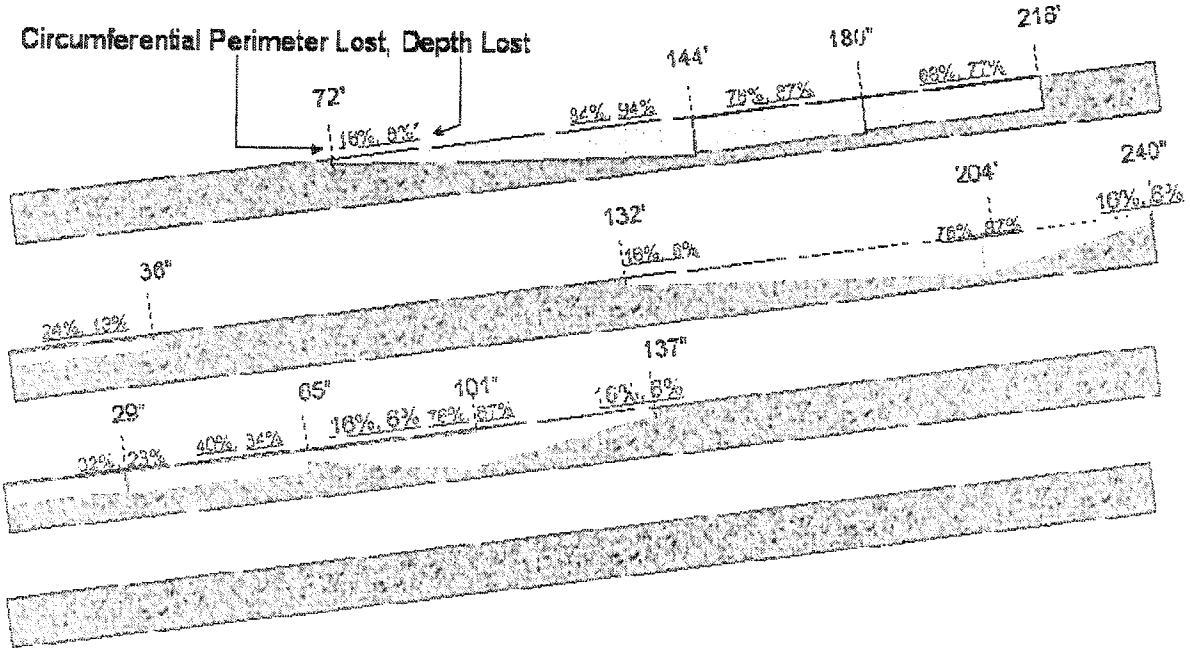

Figure 11 – Design Grout Defects in the South Wall in 4 inch (101.6 mm) Metal Ducts

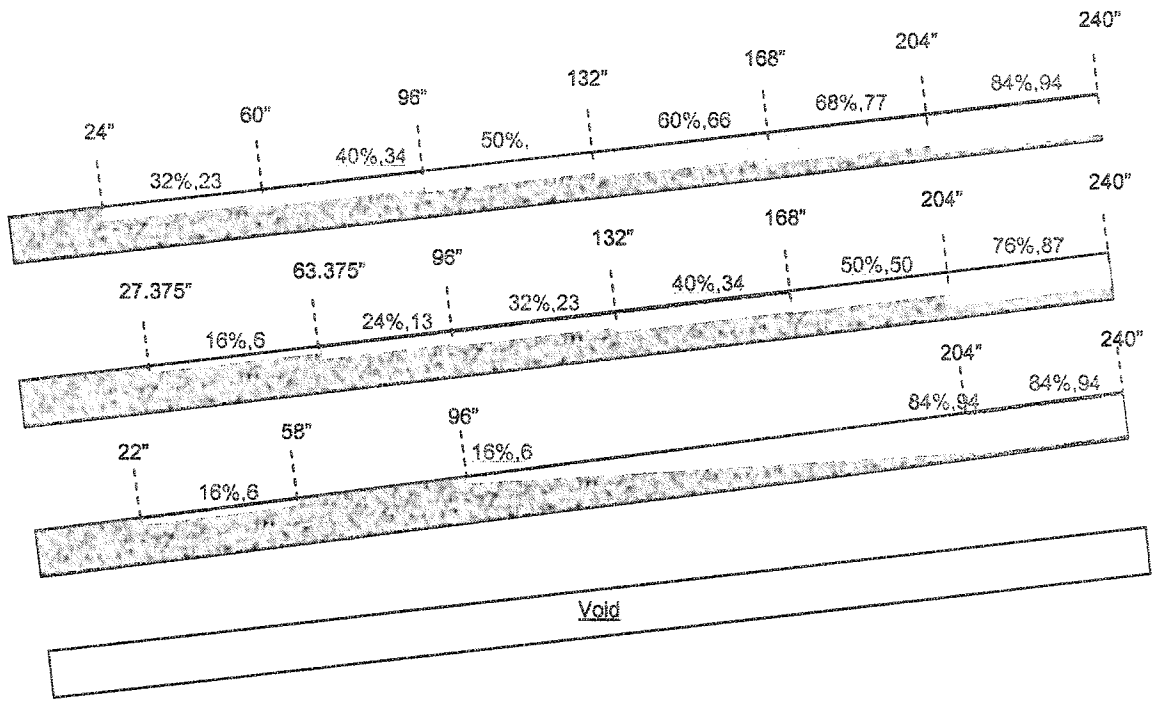

Figure 12 – Design Grout Defects in the North Wall in 4 inch (101.6 mm) Metal Ducts

4.3 Background of Nondestructive Evaluation (NDE) Methods

This section presents brief backgrounds of selected NDE methods used in the research. These methods include Impact Echo, Spectral Analysis of Surface Waves and Ultrasonic Pulse Echo tests.

4.3.1 Impact Echo (IE) Test

The IE test is typically a "point by point" test. The test generally involved impacting one side of the concrete surface with a small solenoid operated impactor and identifying the reflected wave energy with a displacement transducer. The schematic of the IE test is shown in Figure 13. The resonant echoes of the displacement responses are usually not apparent in the time domain, but are more easily identified in the frequency domain. Consequently, the linear frequency spectra of the displacement responses are calculated by performing a Fast Fourier transform (FFT) analysis to determine the resonant echo peak(s). The relationship among the resonant echo depth frequency peak (f), the compression wave velocity (V_P) and the echo depth (D) is expressed in the following equation:

$$D = \beta V_p/(2*f) \qquad (1)$$

where β is a factor equal to from 0.87 for a square column to 0.96 for a slab/wall shape

The IE method can be used for measuring concrete thicknesses, evaluating concrete quality, and detecting hidden flaws such as cracks, honeycombs, etc. The IE method is most sensitive to cracks that are parallel and sub-parallel to the test surface.

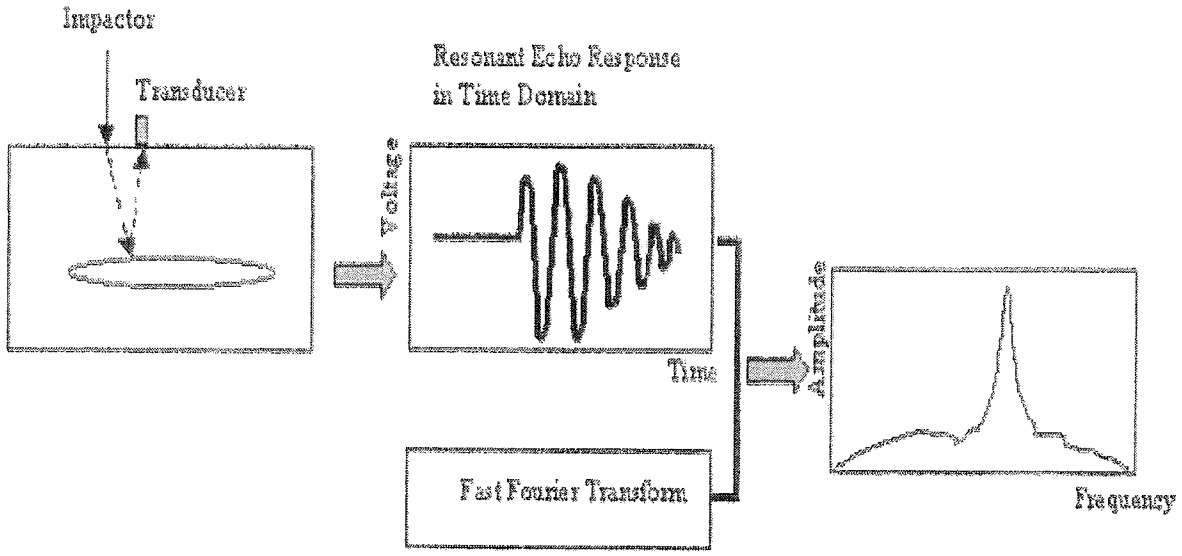

Figure 13 – Schematic of Impact Echo Method

4.3.2 Spectral Analysis of Surface Waves (SASW) Test

The SASW method uses the dispersive characteristics of surface waves to determine the variation of the surface wave velocity (stiffness) of layered systems with depth. The SASW testing is applied from the surface which makes the method nondestructive and nonintrusive. Shear wave velocity profiles can be determined from the experimental dispersion curves (surface wave velocity versus wavelength) obtained from SASW measurements through a process called forward modeling (an iterative inversion process to match experimental and theoretical results). The SASW method can be performed on any material provided an accessible surface is available for receiver mounting and impacting. Materials that have been tested with the SASW method include concrete, asphalt, soil, rock, masonry, and wood.

Applications of the SASW method include, but are not limited to: 1) determination of pavement system profiles including the surface layer, base and subgrade materials, 2) determination of seismic velocity profiles needed for dynamic loading analysis, 3) determination of abutment depths of bridges, and 4) condition assessments of concrete liners in tunnels, and other structural concrete conditions.

The SASW method requires an accessible surface for receiver attachments. The extent of the accessible surface limits the investigation depth. As a rule of thumb, if one is interested in material properties to a depth of D, then the accessible surface should extend in a line of receivers direction to a distance equal to 1.5D, preferably 2D. Figure 14 presents the general field arrangement used in SASW testing. Receiver spacings ranging from 0.25 to +300 ft have been used in the field by our firm to investigate depths from 0.1 ft up to +300 ft.

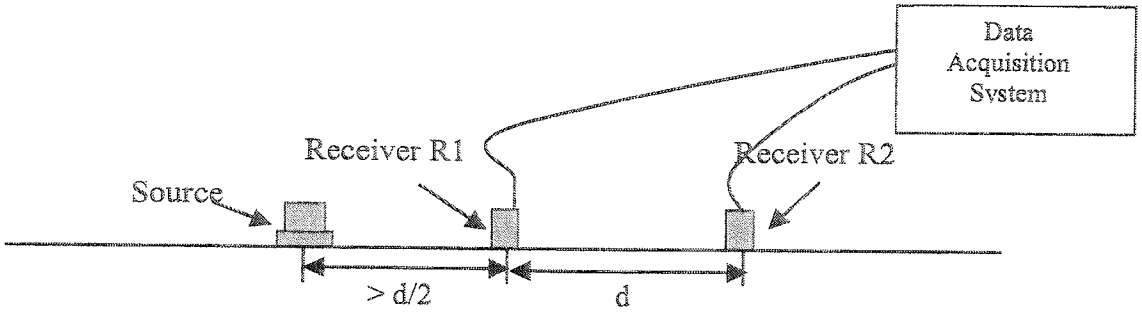

Figure 14 – SASW Test Setup

Elastic Stress Wave Relationships

The following equations from elastic theory illustrate the relationships between shear moduli (G), mass density (ρ, total unit weight divided by gravitational acceleration), shear wave velocity (Vs), Young's modulus of elasticity (E), Poisson's ratio (ν), compression wave velocity (Vp), and constrained modulus (M):

Direct P- or S- Wave Velocity: $Vp = D / tp$ or $Vs = D/ts$ (2)
Shear Modulus: $G = \rho\ Vs^{**}2$ (3)
Young's Modulus: $E = 2\ (1+\nu)\ \rho\ Vs^{**}2 = \rho\ Vp^{**}2\ [(1+\nu)(1-2\nu)/(1-\nu)]$ (4)
Constrained Modulus: $M = \rho\ Vp^{**}2$ (5)
Poisson's Ratio: $\nu = [0.5\ (Vp/Vs)^{**}2 - 1]/[(Vp/Vs)^{**}2 - 1]$ (6)
P- and S-wave Velocities: $Vp = Vs\ [2(1-\nu)/(1-2\nu)]^{**}0.5$ (7)

where D = Distance, tp = P-wave travel time and ts = S-wave travel time.

Values of these parameters determined from seismic measurements (SASW measurements) represent the material behavior at small shearing strains, i.e. strains less than 0.001 percent. Thus, moduli calculated from compression, shear or surface wave velocities represent the maximum moduli of materials because of their low strain levels. It should be noted that the measurement of the surface wave velocity, also called Rayleigh wave velocity, is actually performed in the SASW test. Surface wave velocity (V_R) in a homogeneous half-space is related to shear wave velocity by:

$$V_R \sim 0.9\ Vs \quad (8)$$

(The exact equation is given in numerous geophysical textbooks)

Spectral Analysis of Surface Waves (SASW) Method

Surface wave (also termed Rayleigh; R-wave) velocity varies with frequency in a layered system with differing velocities. This variation in velocity with frequency is termed dispersion. A plot of surface wave velocity versus wavelength is called a dispersion curve.

The SASW tests and analyses are generally performed in three phases: (1) collection of data in situ; (2) construction of an experimental dispersion curve from the field data; and (3) inversion (forward modeling) of the theoretical dispersion curve, if desired, to match theoretical and experimental curves so that a shear wave velocity versus depth profile can be constructed. Wavelength (λ), frequency (f), and wave velocity (Vr), are related as follows:

$$Vr = f^{*}\lambda \quad (9)$$

When the velocity is uniform, the wavelength of the waves is the investigation depth. Forward modeling is most commonly done to determine seismic velocity profiles for earthquake and vibrating machine foundation design purposes.

SASW Experimental Dispersion Curve Processing

The experimental dispersion curve is developed from the field phase data from a given site by knowing the phase (ϕ) at a given frequency (f) and then calculating the travel time (t) between receivers of that frequency/wavelength by:

$$t = \phi / 360^{*}f \quad (10)$$

Surface wave velocity (Vr) is obtained by dividing the receiver spacing (X) by the travel time at a frequency:

$$Vr = X / t \quad (11)$$

The wavelength (λ) is related to the surface wave velocity and frequency as shown in equation 7.

By repeating the above procedure for any given frequency, the surface wave velocity corresponding to a given wavelength is evaluated, and the dispersion curve is determined. The phase data was viewed on the Freedom Data PC (manufactured by Olson Instruments, Inc) system in the field to ensure that acceptable data was being collected. The phase data was then returned to our office for processing. The phase of the cross power spectrum (transfer function) between the two receivers and the coherence function were used in creating the dispersion curves. Coherence is related to signal to noise ratio, and a value near 1.0 indicates good quality data. However, acceptable phase data may have comparatively low coherence.

After masking of all forward and reverse phase record pairs from each receiver spacing, an experimental field dispersion curve is developed that is the plot of surface wave velocity versus wavelength. We used our IES-SASW software to mask the phase data and generate the experimental field dispersion curves presented in the report.

SASW Theoretical Modeling Processing

To determine the shear wave velocity profile from the "apparent" velocities of the dispersion curve, analytical modeling is necessary. The analytical modeling used herein is a forward modeling process that is iterative and involves assuming a shear wave velocity profile and constructing a theoretical dispersion curve. The experimental (field) and theoretical curves are compared, and the assumed theoretical shear wave velocity profile is adjusted until the two curves match using the WINSASW software of the Geotechnical Engineering Center of University of Texas at Austin. The interactive computer algorithm for both 2-dimensional and 3-dimensional analyses have been developed by Dr. Jose Roesset and his colleagues at the University of Texas at Austin to compute a theoretical dispersion curve based upon an assumed shear wave velocity and layer thickness profile. These algorithms have been in use for some time and have produced reasonable accuracy when comparing seismic soil and rock velocities determined with the SASW method with seismic velocities from boring based crosshole or downhole seismic methods.

4.3.3 Ultrasonic Pulse Echo (UPE) Test

Ultrasonic Pulse Echo test is a single sided test method with arrays of sensors using dry acoustic contact. The UPE tests record the echo of the transmitted ultrasonic shear or compressional waves induced by mechanical excitation of the pulsers. The frequency of interest ranges from 33 to 150 kHz. The waves that are introduced into the concrete by the transducer propagate with a certain velocity and are reflected and refracted when the material properties change, or the wave path is interrupted by a void or crack. The reflected energy returns to the transducer and the travel time and amplitude is recorded. The refracted part will continue further into the concrete and perhaps encounter another discontinuity and so forth.

A commercial UPE unit (Low Frequency Flaw Detector – Model A1220 by "SPECTRUM" Moscow Industrial Laboratory, Inc.) was used in this research. The picture of the Low Frequency Flaw Detector is shown in Figure 15. The unit comprises of a control unit and an antenna. The antenna has 24 sensors with 12 sensors used as pulsers and 12 as receivers.

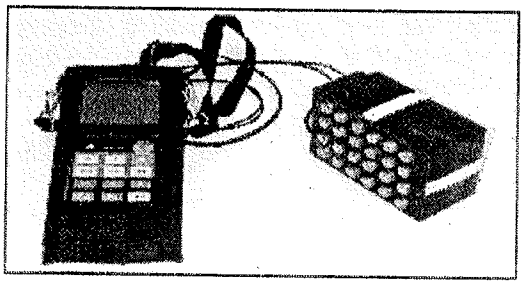

Figure 15 – Low Frequency Flaw Detector (A1220)

5.0 HARDWARE AND SOFTWARE IMPROVEMENTS

Traditional Impact Echo test is based on "point-by-point" basis. The prototype Impact Echo Scanner (IES) was first developed and patented in the mid 1990's by Olson Engineering, Inc. and then used as part of a prestressed concrete cylinder pipe research project for the US Bureau of Reclamation. Four wheels and a rolling displacement transducer were added to the unit (see Figure 1). When the IES test head is rolled across the testing surface, an opto-coupler on the central wheel keeps track of the distance. This unit is calibrated to send an impact at intervals of 1 inch. The IES allows for rapid and near continuous testing. Typical speed of testing with the scanner is 4 meters per minute or 13 ft per minute with impacts applied to the test surface every 1 inch (2.5 cm).

An extra rolling transducer with six displacement transducers was added into the original Impact Echo Scanner. The additional rolling transducer was placed 8 inches (20 cm) apart and in line from the first rolling transducer. This is the first attempt to develop a complete stress wave scanner. Two rolling transducers allow Spectral Analysis of Surface Waves test be performed simultaneously with the Impact Echo test. The Impact Echo test utilizes the data from the

transducer near the impactor while the SASW test uses data from both transducers. Both tests share the same impactor. The open frame photographs of the prototyped IES and IE-SASW scanner are shown in Figures 1 and 2.

Information from the SASW tests can help in condition assessment of internal grout and concrete. Data from the IE and SASW tests can be integrated into a single result for redundancy and to provide the most reliability of the final interpretation of the results. In addition, the surface wave velocity received from the SASW test can be used to calculate the compressional wave velocity used in the IE test based on the above stress wave velocity relationships.

To support hardware improvements, software improvements were added on to the original Impact Echo Scanner software. Multi-channel data acquisition capability was added to acquire data from the second rolling transducer. The three dimensional surface plot was added to the software to view the apparent IE thickness results. The 3-D imaging feature later was discovered to be very helpful in interpretation and visualization of small grout defects. In addition, analysis functions for SASW data were implemented in the software.

6.0 TEST RESULTS

This section includes the SASW and IE test results from the mock-up slab located at BAM facility and the IE and UPE test results from the pre-cast bridge girder. The descriptions of the slab and bridge girder are included in Sections 3.2.1 and 3.2.2. Section 6.1 presents the interpretation of data from the tests. The actual results from each duct from the mock-up slab are discussed in Section 6.2. Finally, the test results from the full scale bridge girder are presented in Section 6.3.

6.1 Data Interpretation

6.1.1 Impact Echo Data Interpretation

Localization of grouting discontinuities through Impact Echo Scanning in the mock-up slab and girder was based on an analysis of variations in the impact-echo frequency. A direct echo from the void or duct wall, measured as an impact-echo frequency corresponding to the depth of the discontinuity (given by the formula $D = \beta V_p/2f$ where βV_P = factored compressional wave velocity and f = frequency), has not yet been observed with the scanner. The only IE-based indication of the presence of well-grouted, filled tendon ducts is the apparent minor increase in apparent wall thickness over such a duct (typically on the order of 12.7 mm or 0.5 in or less). Grouting defects cause a much more significant increase of the apparent wall thickness in IE results as shown herein. This is in accordance with the interpretation of the impact-echo signal as a resonance effect, rather than a reflection of a localized acoustical wave. The shift in the IE thickness indicating grout voids can be seen most clearly in a three-dimensional surface plot. Figures 16a and 16b present frequency spectrums of the two extreme cases: a fully grouted duct and a completely voided duct. The frequency peak was observed at 6,445 Hz for the completely grouted duct. This results in an IE thickness of 11.17 inches. However, the frequency peak shifted to 5,274 Hz and resulted in an increase in the IE thickness to 13.65 inches for a test of a completely voided duct. This is a 20% decrease in the frequency peak with a corresponding increase in the IE thickness.

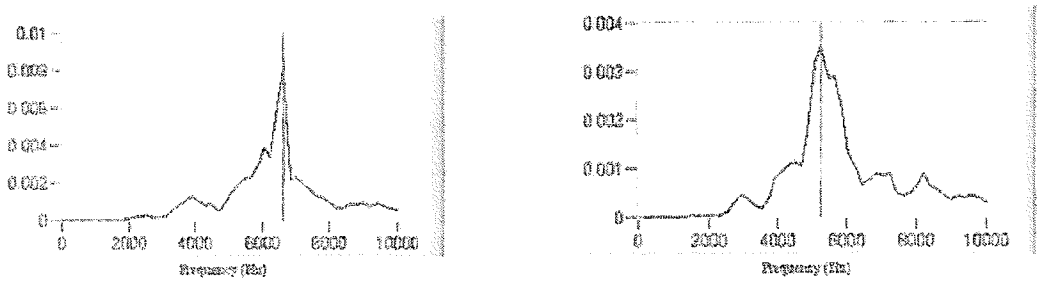

Figures16a and 16b – Spectrum from U-Shaped Girder 4 inch ducts with good grout condition (left) and no grout condition (right)

6.1.2 Spectral Analysis of Surface Waves Data Interpretation

The determination of grout defects was based on reductions of surface wave velocity. A surface wave velocity in area with well grouted duct is approximately 8,000 ft/sec. The surface wave velocity reduced to approximately 7,100 ft/sec in areas with grout voids at the BAM slab. This is an 11.25% reduction in the surface wave velocity value.

6.1.3 Ultrasonic Pulse Echo Data Interpretation

Data from Ultrasonic Pulse Echo tests are typically analyzed in the time domain. Typically an envelope of the time domain data is used in the reflection analysis. This envelop of the time domain data is sometime called an A-scan which is data from a single test. An example of an A scan with the amplitude of the data converted to greyscale is shown in Figure 17 for a shear wave pulse echo. If the characteristic wave velocity of the concrete is known then the travel time can be converted to depth/thickness.

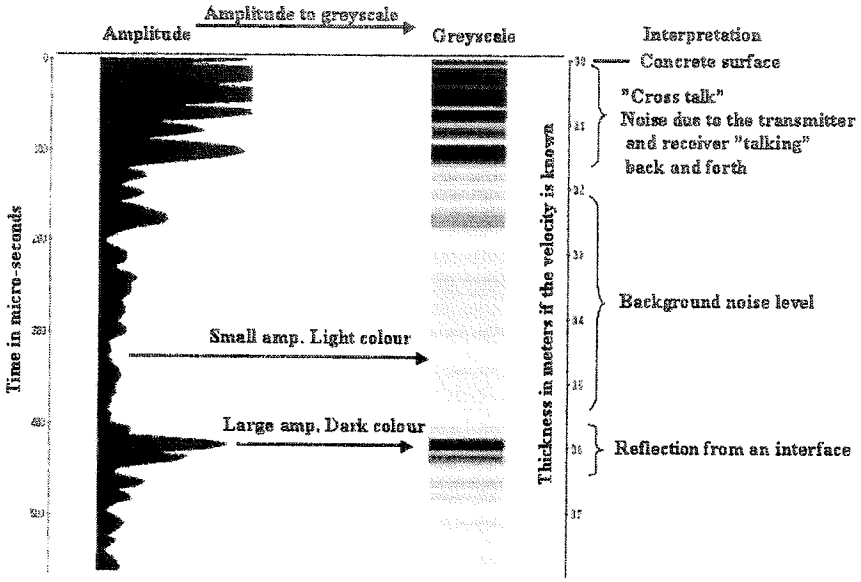

Figure 17 – An Example of A Scan data (from FORCE INSTITUTE)

The UPE test is generally performed in a grid or line format with the source/receiver unit moved to a new position and another A-scan is recorded. A number of A-scans comprise a profile or B-scan of the internal echoes. The B-scan is usually presented as a gray-scale diagram in which the amplitudes are reflected by the tone of the gray level. A result indicative of a potential grout defect is a shallow echo with an absence of the back wall echo.

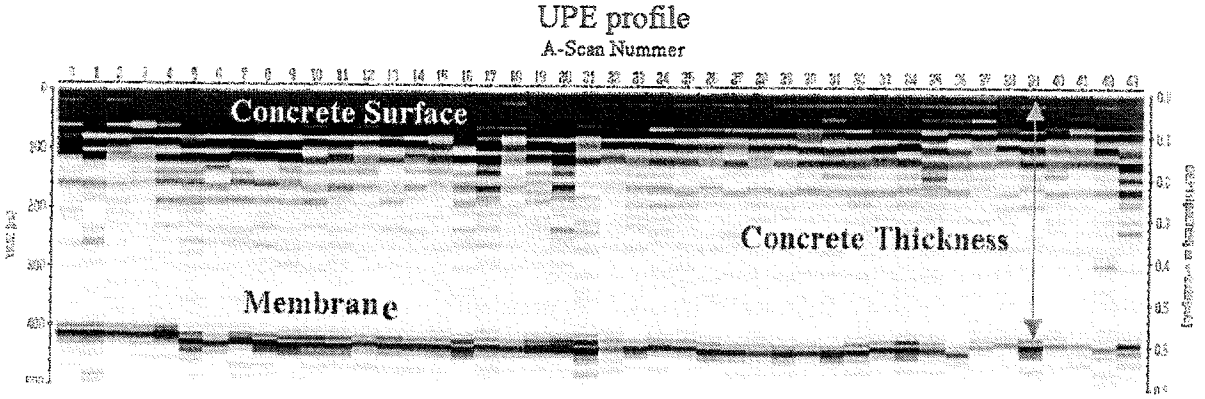

Figure 18 – An Example of B Scan data (data from FORCE INSTITUTE)

6.2 Results from the Mock-up Slab (at BAM facility)

A stress wave scanner was used on the mock-up wall to perform the Impact Echo Scanning simultaneously with the Spectral Analysis of Surface Waves tests. The tests were performed every 5 cm in a line fashion parallel to the direction of the ducts across the 13 ft (4 m) wide slab. A total of 200 scan lines were performed on this specimen. Figure 19 depicts a traditional way to analyze the Impact Echo data. Time domain data is recorded from a transducer. Then Fast Fourier Transform (FFT) was applied to the data in the time domain to obtain the linear displacement frequency spectrum. A dominant frequency is selected to back calculate for the IE thickness. The IE thickness can then be plotted together in a line (left plot in Figure 19) versus scan distance.

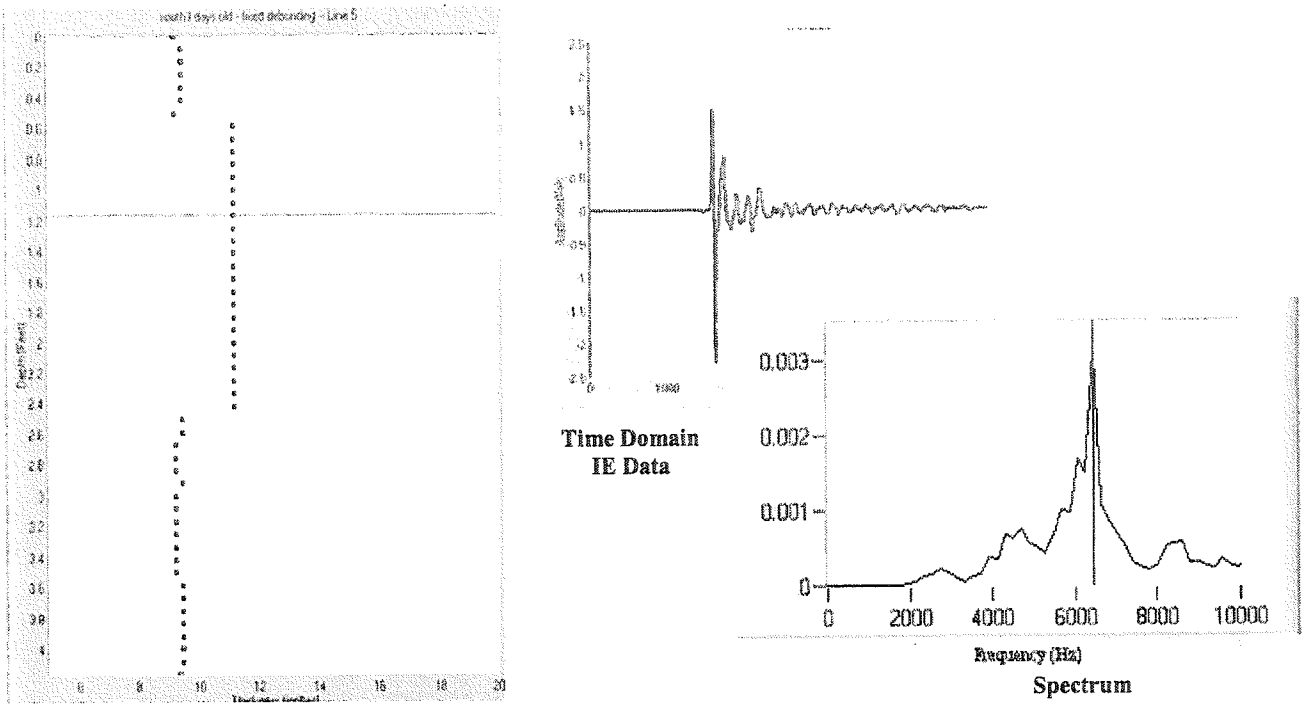

Figure 19 – Traditional Impact Echo Analysis

A new way of analysing the Impact Echo data is to assemble IE thickness data from all the scan lines together to generate a three dimensional surface plot. An example of a 3D surface plot is shown in Figure 20. Review of Figure 20 shows areas with varying thickness due to embedded Styrofoam in the slab.

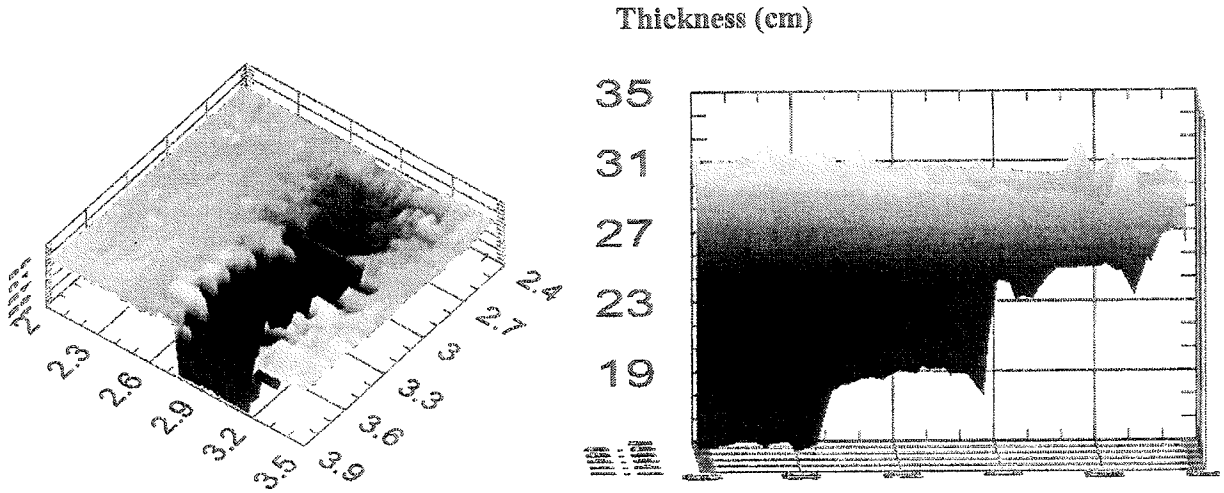

Figure 20 – An Example of a 3D Surface Plot of IE Thickness of the Mock-up Slab and the thickness profile

6.2.1 IES Results from the Duct Area from the BAM Mock-up Slab

The main focus of the research is condition evaluation of the internal grout conditions. The initial analysis of the IES tests was performed on the mock-up slab and completed without prior knowledge of actual defect design. A 3D example of the IE thickness plot of an area with ducts is presented in Figure 21. BAM requested the exact location of the defects in the slab to remain confidential so that other organizations can use the specimen for blind studies in the future. Consequently, however, the comparison of the test results and actual defect design can be carried out without specifying the exact location of the duct in the slab. Review of Figure 21 shows 7 ducts inside the mock-up slab. Note that the thicker portions represent grout void. Zoomed in results of individual duct with its actual defect design are also included in this section. However, the results presented herein are not in the order of the ducts inside the slab.

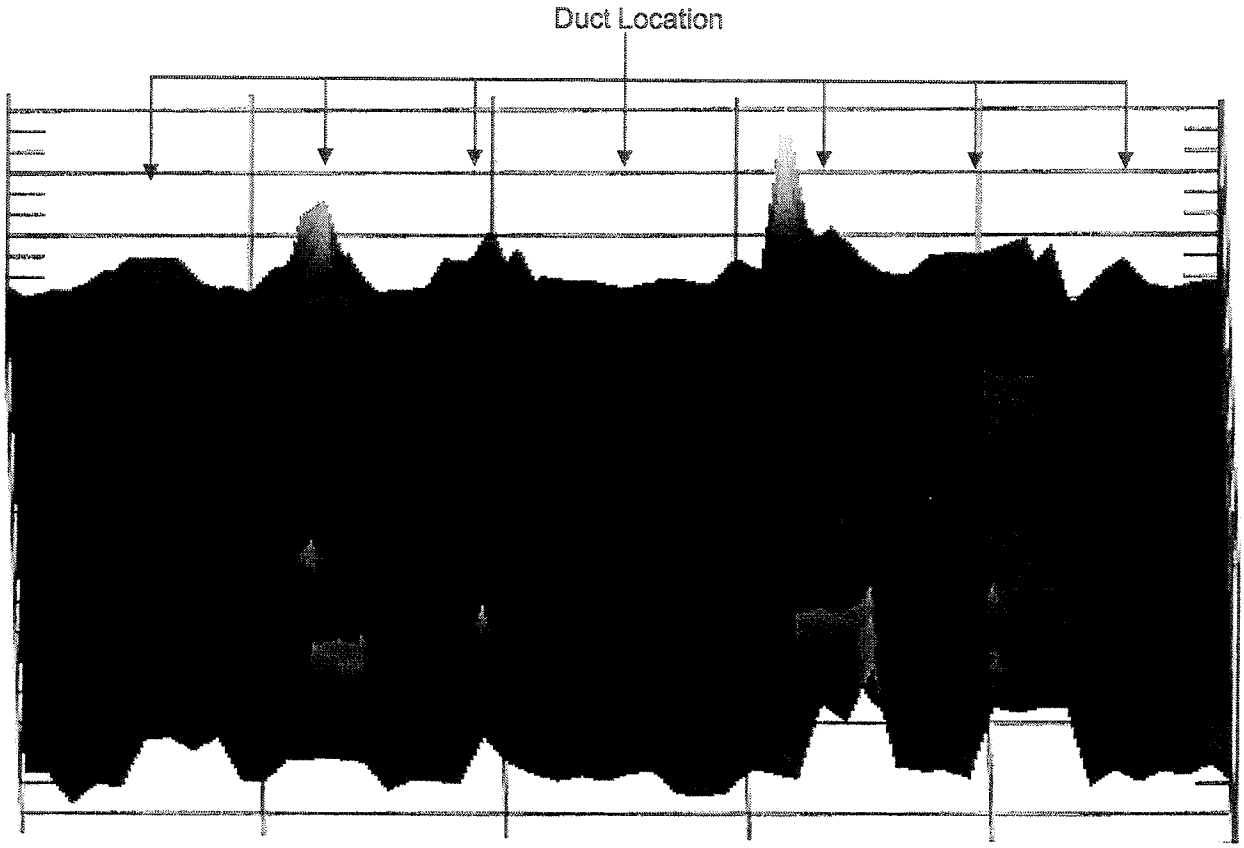

Figure 21 – Example of the 3D IE Thickness Plot from the Duct Area

Duct A: The zoomed-in 3D surface plot of the IES thickness result from Duct A and its actual defect design are presented in Figure 22. The diameter of Duct A is 120 mm or 4.72 inches with concrete cover of 70 mm or 2.76 inches. Figure 22 shows a 3D surface plot of the IE thickness from Duct A in the top picture. The middle picture in Figure 22 shows an interpretation of the IE results in the top picture and the bottom picture in Figure 22 is the actual defect design. Reviews of Figure 22 show half diameter grout void (Defect A) was detected and complete grout voids (Defects B and C) were also detected. However, the IE test result shows more defects than the actual defect design. The IE result shows grout defects toward the right end of the duct where grout defects were not intended to be at the location. This may be due to local debonding between the grout and metal duct at that location. In addition, the IE results cannot identify the difference between the silicone contamination on the outside of a duct (to simulate debonding) and actual grout defects.

Duct B: The zoomed-in 3D surface plot of the IES thickness result from Duct B and its actual defect design are presented in Figure 23. The diameter of Duct B is 100 mm or 3.94 inches with concrete cover of 80 mm or 3.15 inches. Review of Figure 23 shows half diameter grout void (Defect A) was detected and complete grout voids (Defects B and C) were also detected. However, the IES test result shows more defects than the actual defect design. The IES result shows grout

defects toward the right end of the duct where grout defects were not intended to be at the location. Again, this is probably the result of local debonding between grout and duct at that location or an unintended grout defect.

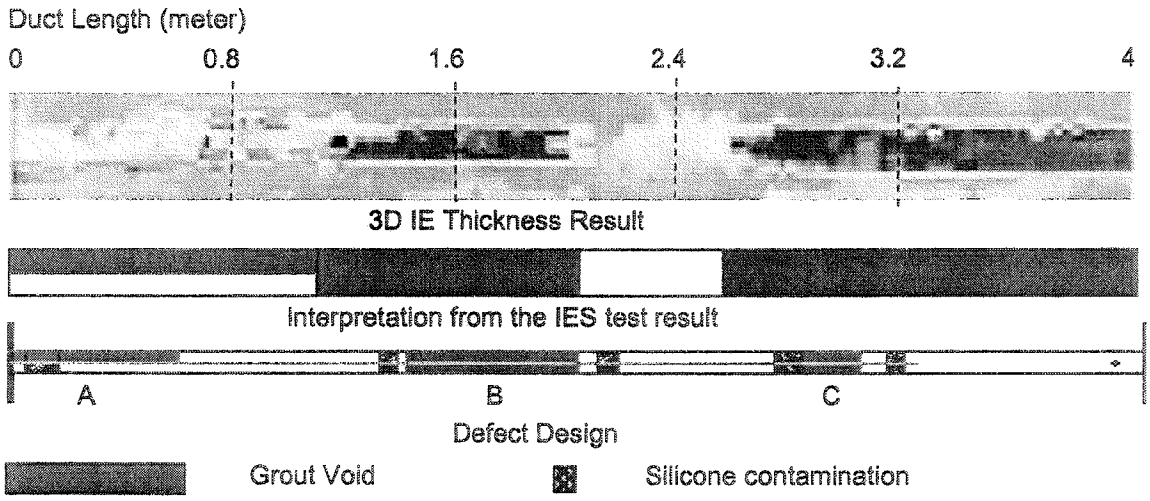

Figure 22 – Comparison of IES Test Results (and its interpretation) and the Actual Defect Design – Duct A

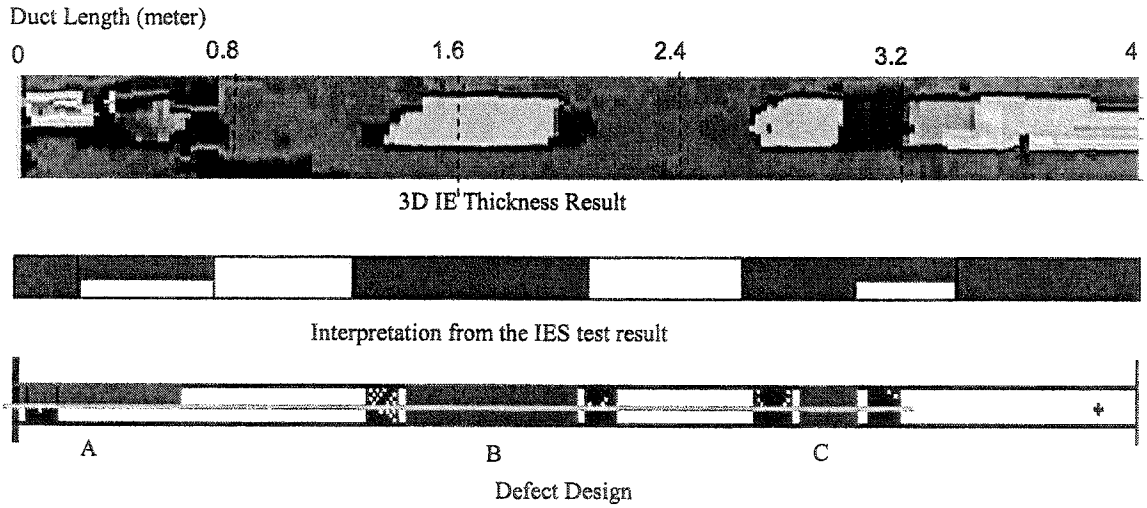

Figure 23 – Comparison of IES Test Results (and its interpretation) and the Actual Defect Design – Duct B

Duct C: The zoomed-in 3D surface plot of the IES thickness result from Duct C and its actual defect design are presented in Figure 24. The diameter of Duct C is 80 mm or 3.15 inches with concrete cover of 170 mm or 6.7 inches. Review of Figure 24 shows half diameter grout void (Defect A) was detected and a complete grout void (Defect C) was also detected. However, the interpretation of the IES test result indicated a half diameter grout defect instead of a full diameter void (Defect B). The IE result shows grout defects toward the right end of the duct and locations where silicone contaminations were applied.

Duct D: The zoomed-in 3D surface plot of the IE thickness result from Duct D and its actual defect design are presented in Figure 25. The diameter of Duct D is 80 mm or 3.15 inches with concrete cover of 140 mm or 5.5 inches. The interpretation of the IES test result indicates half diameter grout defects instead of full diameter void for Defects A and B. In addition, only part of the half diameter void (Defect C) was detected in this case. The interpretation of the grout defect shows apparent false positives in some areas.

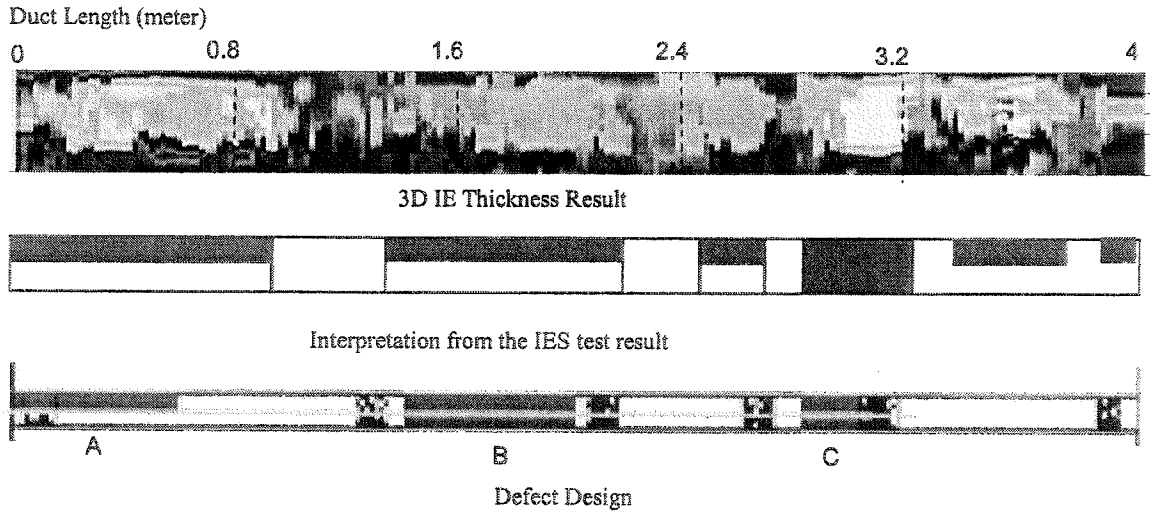

Figure 24 – Comparison of IES Test Results (and its interpretation) and the Actual Defect Design – Duct C

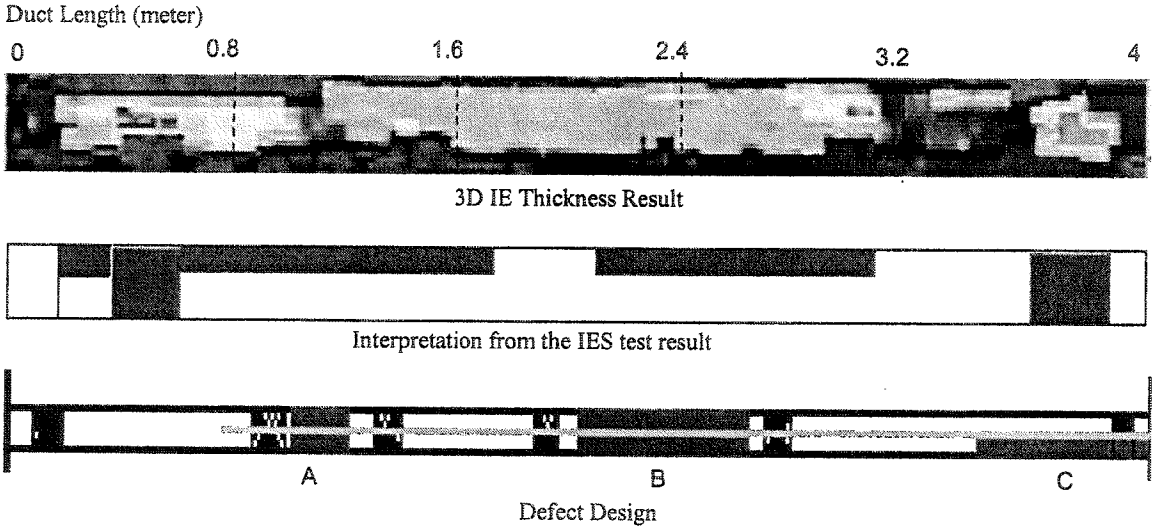

Figure 25 – Comparison of IES Test Results (and its interpretation) and the Actual Defect Design – Duct D

Duct E: The zoomed-in 3D surface plot of the IE thickness result from Duct E and its actual defect design are presented in Figure 26. The diameter of Duct E is 80 mm or 3.15 inches with concrete cover of 100 mm or 3.94 inches. Reviews of Figure 26 show that part of the half diameter grout void (Defect A) was not detected. Complete grout voids (Defects B and C) were detected in this case. However, the interpretation of the IE test result indicates half diameter grout defect instead of full diameter void (Defect B). Also, the interpretation of the grout defect shows false positives in some areas

Duct F: The zoomed-in 3D surface plot of the IE thickness result from Duct F and its actual defect design are presented in Figure 27. The diameter of Duct F is 60 mm or 2.36 inches with concrete cover of 100 mm or 3.94 inches. Reviews of Figure 27 show that the half diameter grout void (Defect A) was not detected. Complete grout voids (Defects B and C) were detected in this case. However, the interpretation of the IE test result indicates half diameter grout defect instead of full diameter void (Defect B).

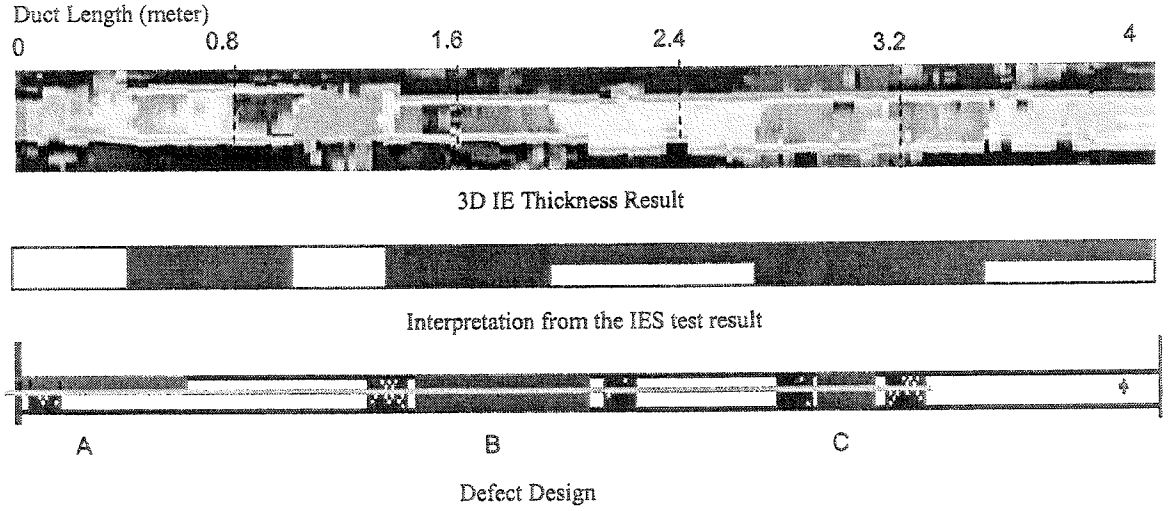

Figure 26 – Comparison of IES Test Results (and its interpretation) and the Actual Defect Design – Duct E

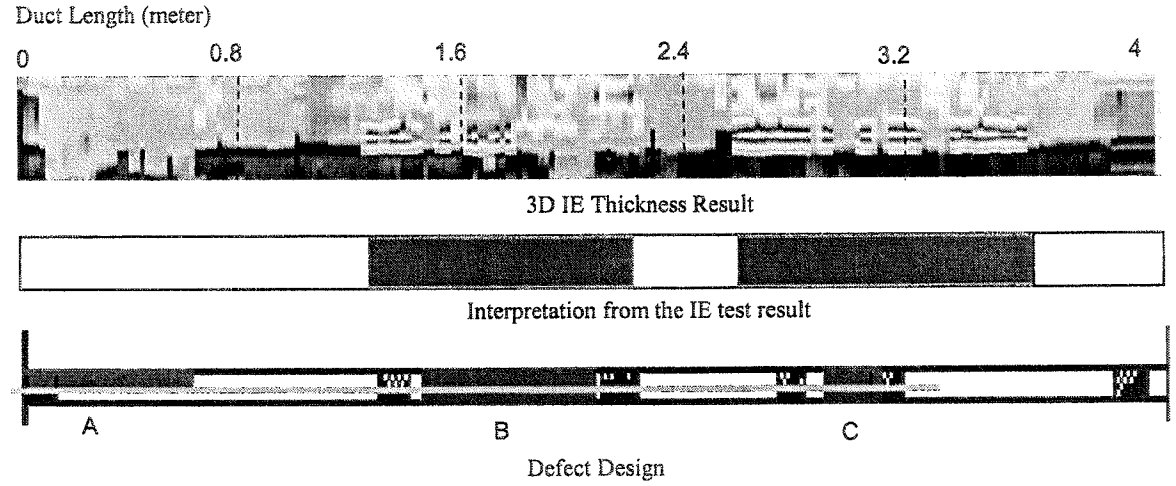

Figure 27 – Comparison of IES Test Results (and its interpretation) and the Actual Defect Design – Duct F

Duct G: The zoomed-in 3D surface plot of the IE thickness result from Duct G and its actual defect design are presented in Figure 28. The diameter of Duct G is 40 mm or 1.57 inches (the smallest diameter used in the mock-up slab) with concrete cover of 110 mm or 4.33 inches. Review of Figure 28 shows that half diameter grout void (Defect A) was not detected. Complete grout voids (Defects B and C) were detected in this case. However, the interpretation of the IE results shows false positives in some areas.

Duct H: The zoomed-in 3D surface plot of the IE thickness result from Duct H and its actual defect design are presented in Figure 29. The diameter of Duct H is 40 mm or 1.57 inches (the smallest diameter used in the mock-up slab) with concrete cover of 170 mm or 6.7 inches. Review of Figure 29 shows that half diameter grout void (Defect A) was correctly identified. Full diameter grout voids (Defects B and C) were also detected in this case. However, the interpretation of the IE results shows false positive in many areas.

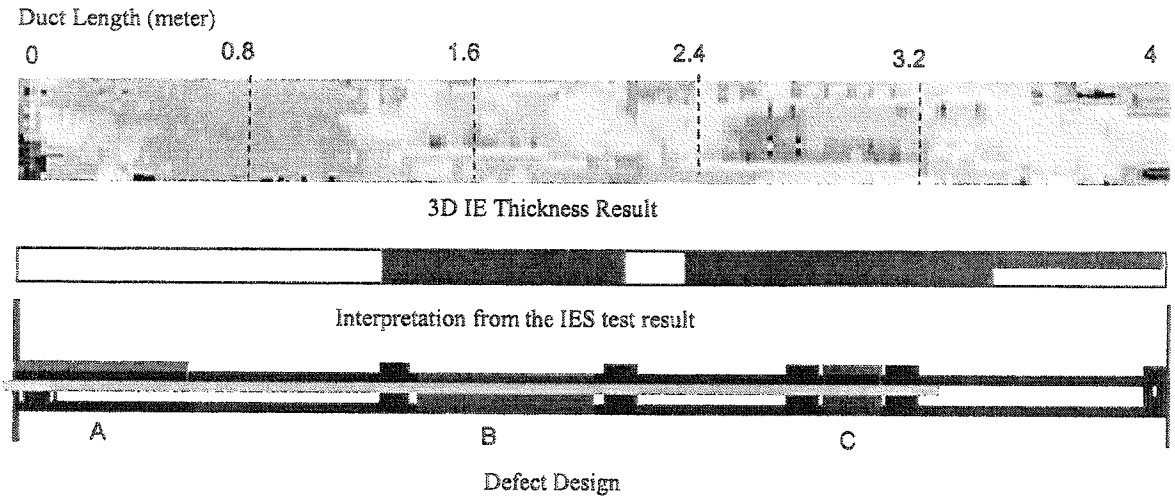

Figure 28 - Comparison of IES Test Results (and its interpretation) and the Actual Defect Design – Duct G

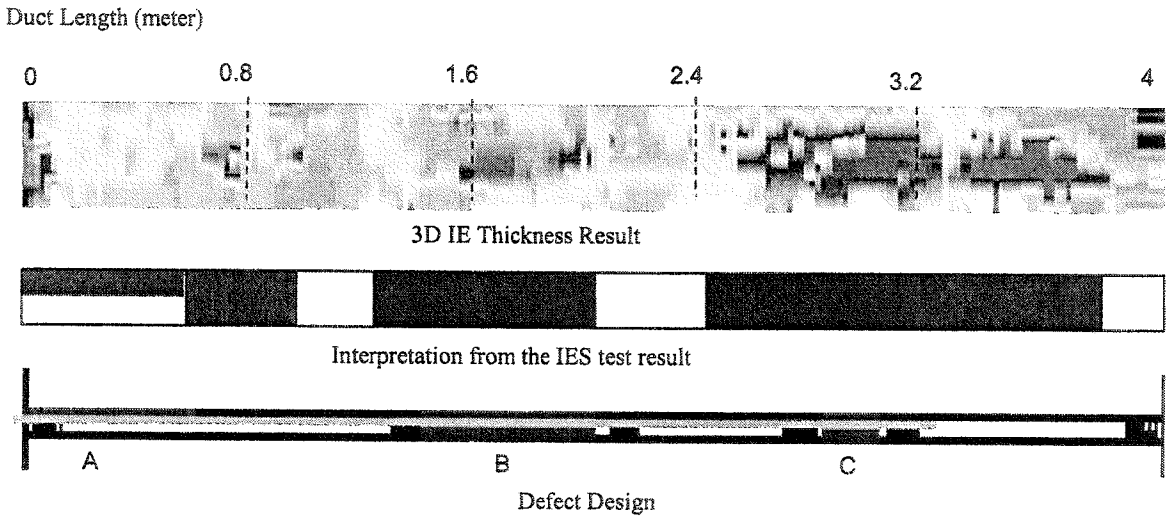

Figure 29 - Comparison of IES Test Results (and its interpretation) and the Actual Defect Design – Duct H

Duct I: The zoomed-in 3D surface plot of the IE thickness result from Duct I and its actual defect design are presented in Figure 30. The diameter of Duct I is 40 mm or 1.57 inches (the smallest diameter used in this study) with concrete cover of 190 mm or 7.48 inches (the deepest concrete cover used in the mock-up slab) Review of Figure 30 shows that neither the half diameter grout void (Defect C) nor full diameter grout void was correctly identified.

Duct J: The zoomed-in 3D surface plot of the IE thickness result from Duct J and its actual defect design are presented in Figure 31. The diameter of Duct J is 40 mm or 1.57 inches (the smallest diameter used in this study) with concrete cover varying from 50 to160 mm or 1.97 to 6.3 inches. The concrete cover is deeper toward to left end. Review of Figure 31 shows that half diameter grout void (Defect A) was not detected where the concrete cover is the highest. The IE test was able to identify full diameter grout defect (Defects B and C). In addition, the IE result shows grout defects toward the right end of the duct where grout defects were not intended to be at the location

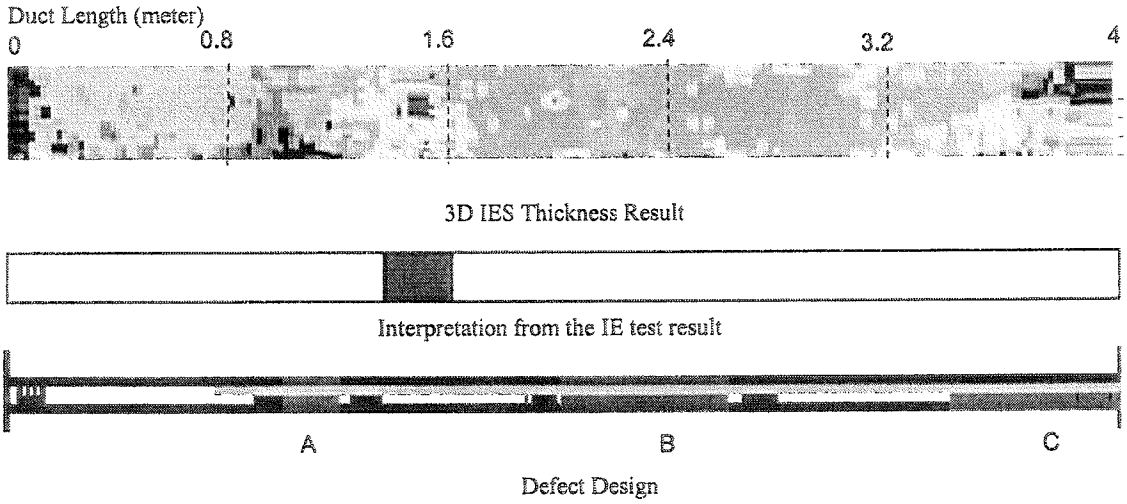

Figure 30 - Comparison of IES Test Results (and its interpretation) and the Actual Defect Design – Duct I

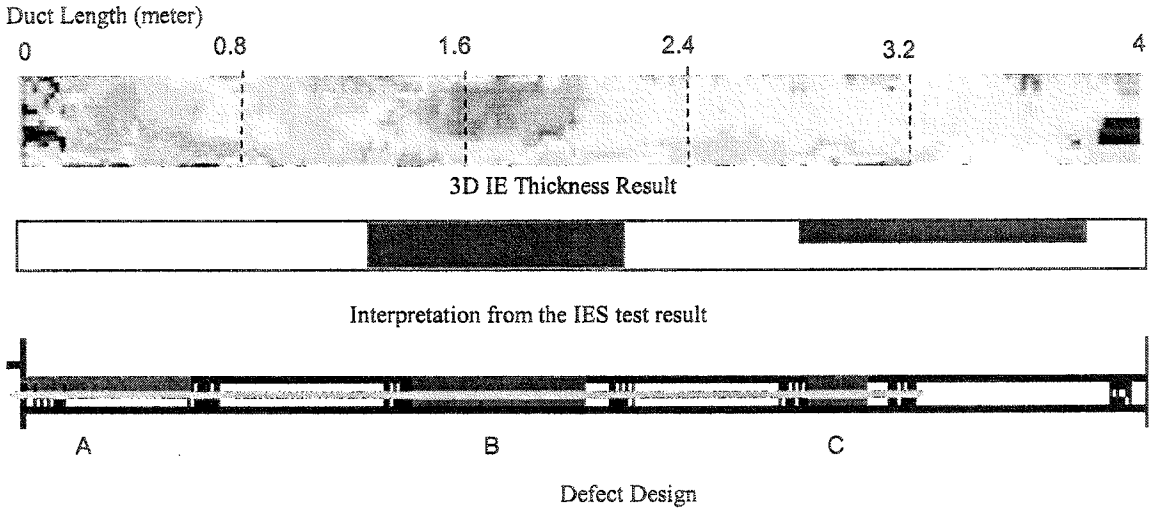

Figure 31 - Comparison of IES Test Results (and its interpretation) and the Actual Defect Design – Duct J

6.2.2 SASW Results from the BAM Duct Area

As stated earlier in the report that this is the first attempt to develop a complete stress wave scanner, the research team experienced some technical issues with the second rolling transducer. Data obtained from the second rolling transducer were intermittent due to varying contact conditions between the transducer and the test surface. This section presents an example of SASW data from a scan. The scan was performed directly on top of Duct A (diameter = 120 mm or 4.72 inches with concrete cover of 70 mm or 2.76 inches). Review of Figure 32 shows that the surface wave velocity reduced from approximately 8000 ft/sec at locations with completely filled duct to 7100 – 7400 ft/sec in the areas with complete voids inside the duct. This is approximately a 7 – 11% reduction in surface wave velocity.

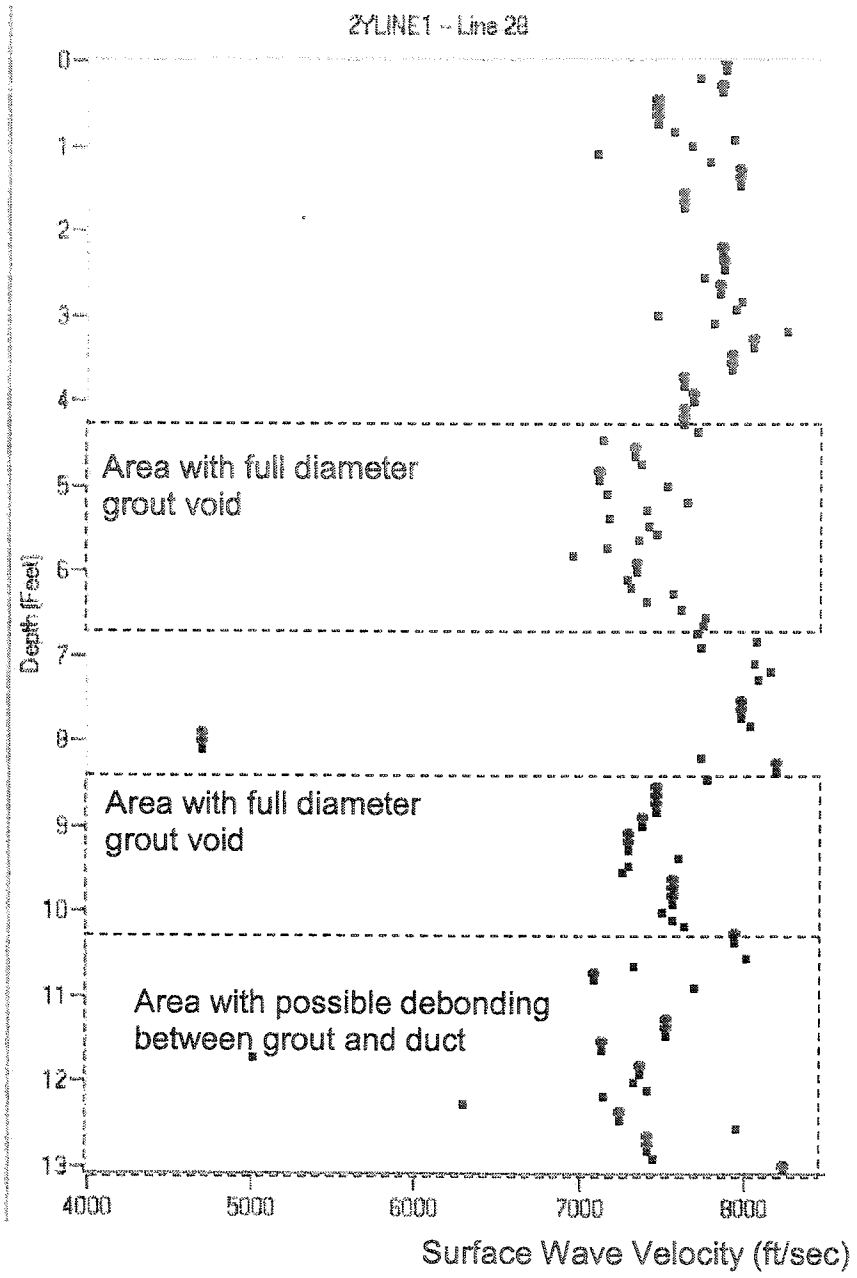

Figure 32- Results from SASW tests directly on top of Duct A (diameter = 120 mm or 4.72 inches with concrete cover of 70 mm or 2.76 inches)

6.3 Results from the Full Scale U-Shaped Bridge Girder

A scanner with one rolling transducer for IES testing was used to test the U-Shaped bridge girder. The IE results are presented in 3D surface plot fashion and are included in Section 6.3.1. In addition, Ultrasonic Pulse Echo (UPE) tests using a commercial device (Low Frequency Flaw Detector – A1220 by "SPECTRUM" Moscow Industrial Laboratory, Inc.) were performed on the south wall of the girder. The UPE tests were performed in a grid format with resolution of 6 inches along the length of the wall by 2 inches along the height of the wall. The results from the UPE test are included in Section 6.3.2.

6.3.1 Impact Echo Test Results

The IE tests were performed in a line fashion every 6 inches vertically across four ducts. Forty test lines were performed on each wall. The two web walls of the girder are referred as the South Wall and North Wall in this report. An example IE thickness result from the South Wall in a skewed 3D surface plot is shown in Figure 33. The IES result in plan view is presented in Figure 34a with the color scale in Figure 34b. The normalized IE thickness (IE thickness results/nominal thickness of the wall) result from the North Wall is presented in Figure 35a with the color scale in Figure 35b. The X scale of the 3D surface plot of the IE thickness in Figures 34 and 35 is the length of the wall and the Y scale is the height of the wall. Comparisons of the IE results and the actual defect designs are also included in this section.

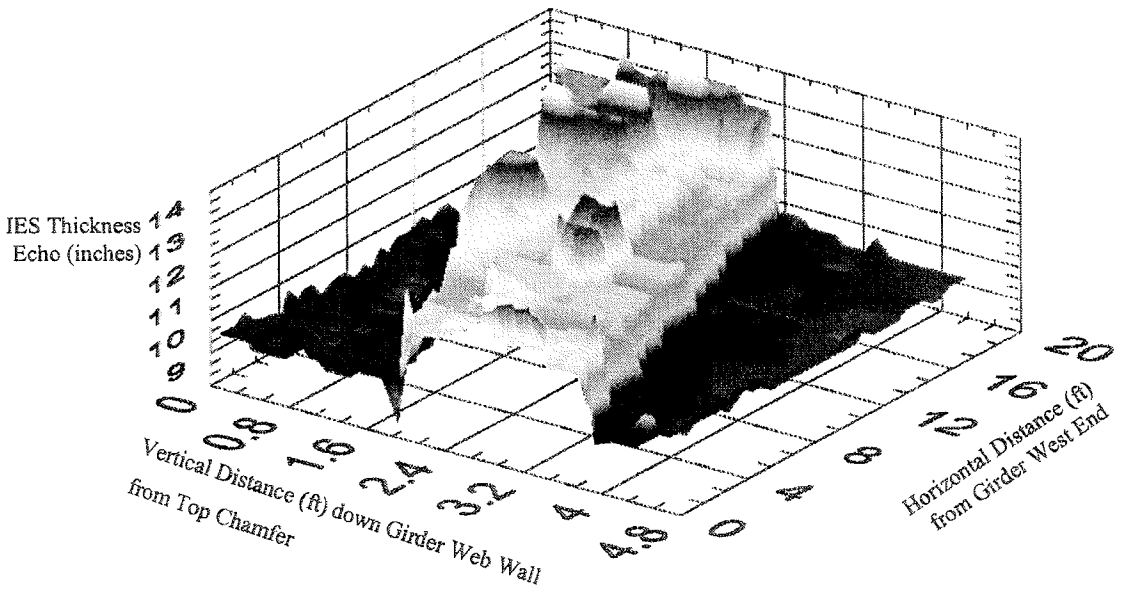

Figure 33 – 3D Surface Plot (Skewed) from the IES results from the South Wall

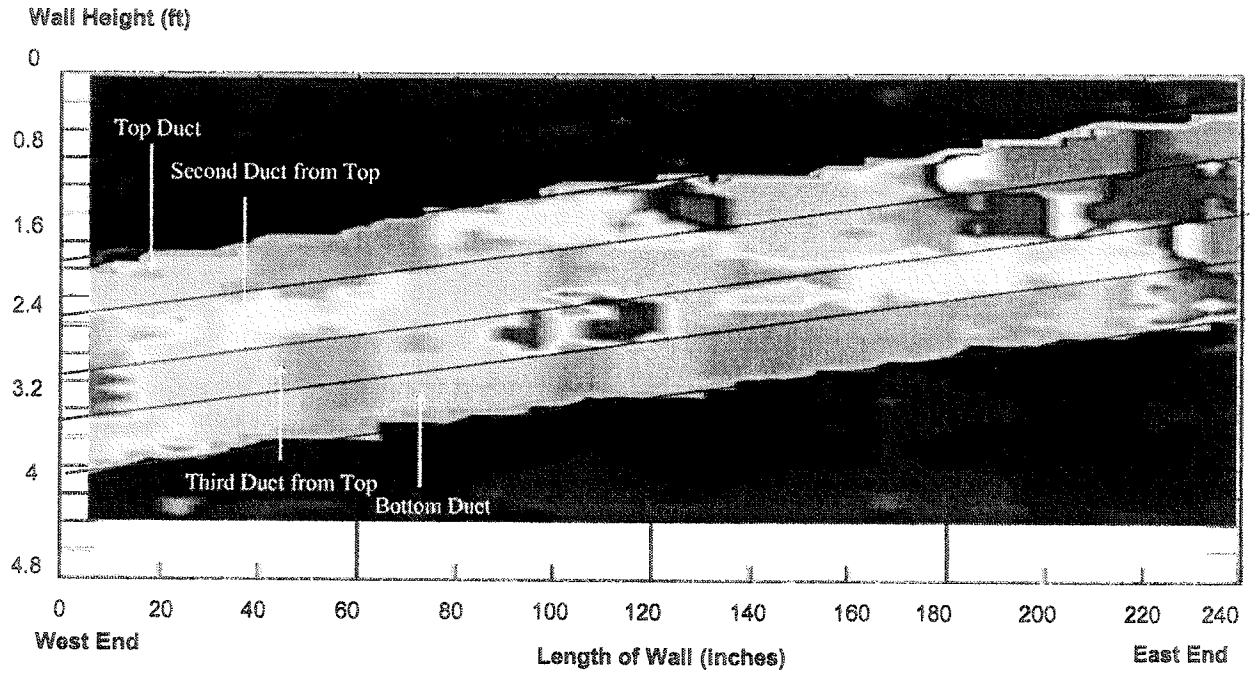

Figure 34a – 3D Surface Plot of IE Thickness Results from the South Wall

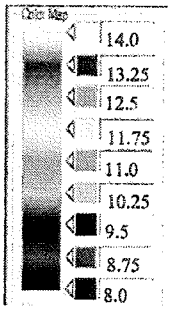

Figure 34b – Color Scale for the IES test results from South Wall in inches thickness

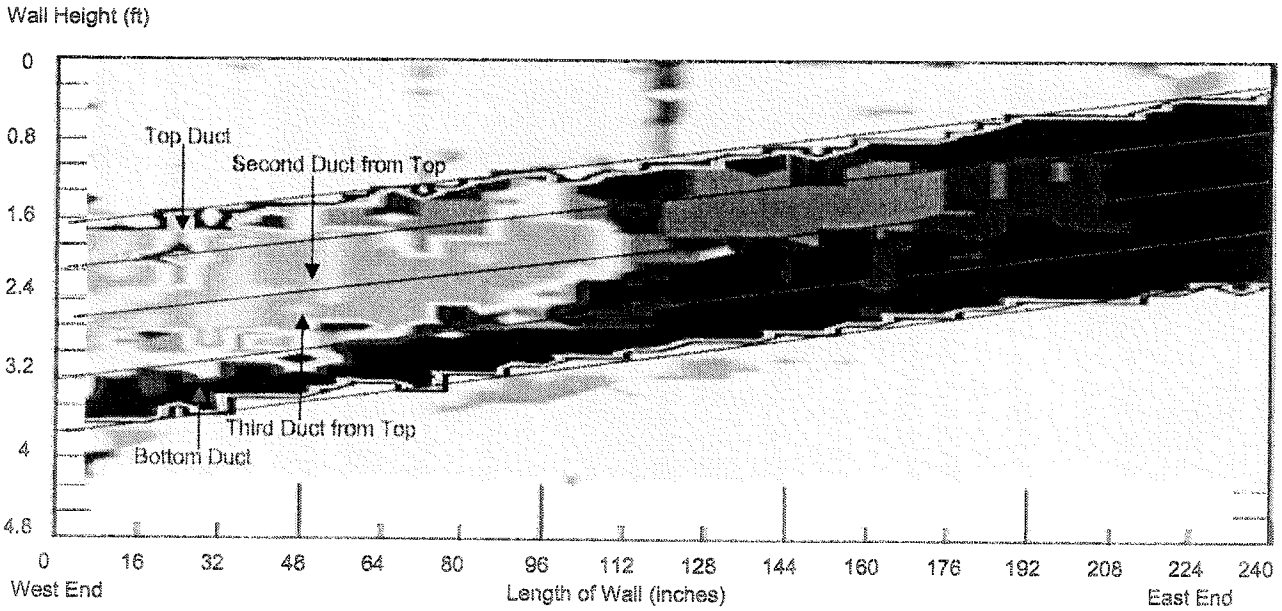

Figure 35 – 3D Surface Plot of IE Thickness Results from the North Wall

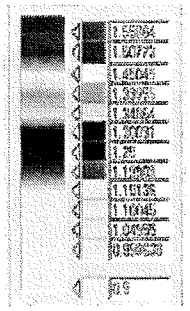

Figures 35b– Color Scale for the IE Results from North Walls (Normalized to 10 inch Wall Thickness)

Comparisons of the IE results and the defect design of South Wall

Top Duct: A comparison of the IES test results from the top duct of the South wall and its defect design (placed above the results from the top duct) is presented in Figure 36. A taper defect was used with the smallest grout void of 16% circumferential perimeter lost or 6% depth lost. Two additional pieces of Styrofoam were also used toward the east end. Reviews of Figure 36 show a slight change in colour from green to yellow at a length of 76 inches from the west end. This location corresponds to a grout defect of 20% circumferential perimeter lost or 11% depth lost. The grout defect becomes very apparent at a length of 115 inches from the west end. This corresponds to a grout defect size of 57% lost in perimeter or 59% depth lost. A grout defect also is apparent toward the east end of the duct. Note that the east end of all four ducts experienced mechanical disturbance when 4" cores were drilled for grout injection outlets.

Second Duct from Top: A comparison of the IES test results from the second duct from top of the South wall and its defect design (placed above the results from the second duct from top) is presented in Figure 37. Two sections of tapered Styrofoam grout defect were used with the smallest grout void of 16% circumferential perimeter lost or 6% depth lost to the largest of 76% perimeter lost or 87% depth lost. An additional piece of Styrofoam was used at the west end to simulate grout defect size of 24% perimeter lost or 13% depth lost. Review of Figure 37 indicates that a grout defect occurs at the west end. This location corresponds to a grout defect of 24% perimeter lost or 13% depth lost. In addition, a minor grout defect was also detected where no Styrofoam is placed near the first detected grout defect. Then grout defects appear again at a length of 135 inches from the west end. This location corresponds with a grout defect of 24% perimeter lost or 13% depth lost. Figure 36 shows the worst defect area (in white color) at the location that the biggest Styrofoam was placed.

Third Duct from Top: A comparison of the IE test result from the third duct from top of the South wall and its defect design (placed above the results from the third duct from top) is presented in Figure 38. There were some difficulties placing the Styrofoam in this duct. A piece of foam broke off during the placement of Styrofoam. Therefore there is limited knowledge of actual locations of grout defects inside this duct. Reviews of Figure 38 show grout defect at the west end of the duct. Grout defects were also detected from lengths of 84 – 126 inches from the west end where taper Styrofoams were located. Then grout defect was detected all the way towards the east end of the duct.

Bottom Duct: The results from the bottom duct are included in Figure 39. There are no artificial voids inside the duct and the IE results show that no grout defect was detected except the last 2 feet toward the east end (due to debonding from mechanical disturbance from the core drills).

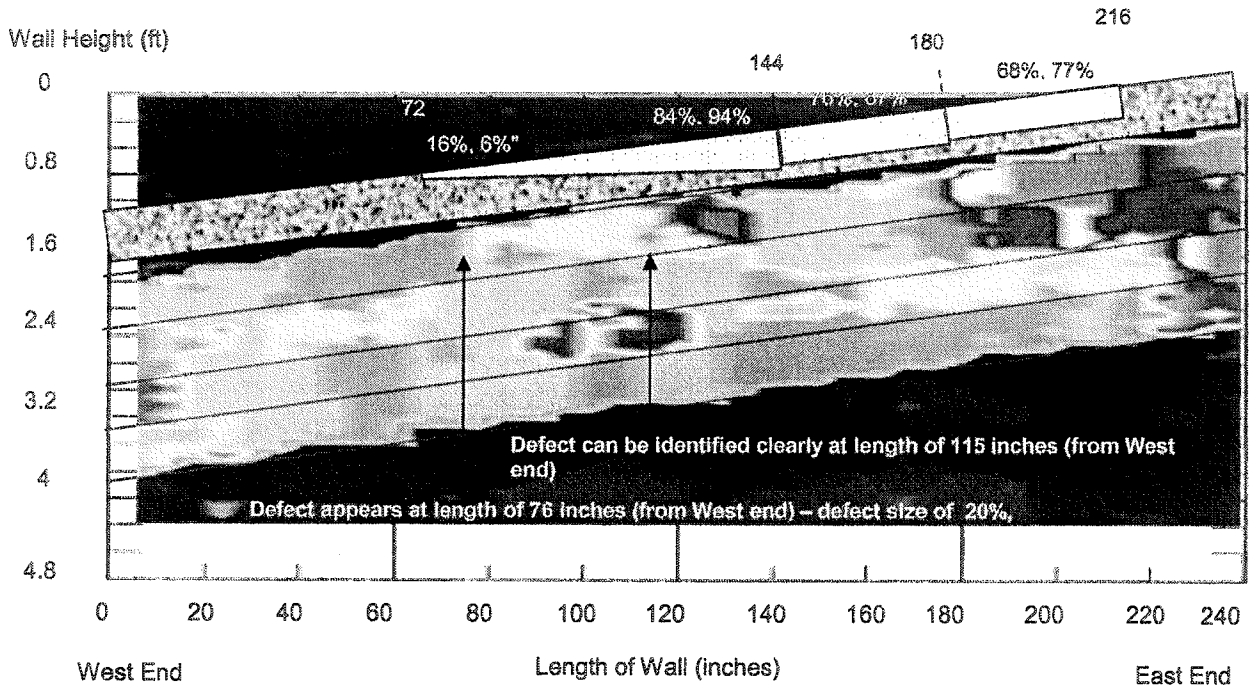

Figure 36 – Comparison of IR results from Top Duct (South Wall) and the Defect Design

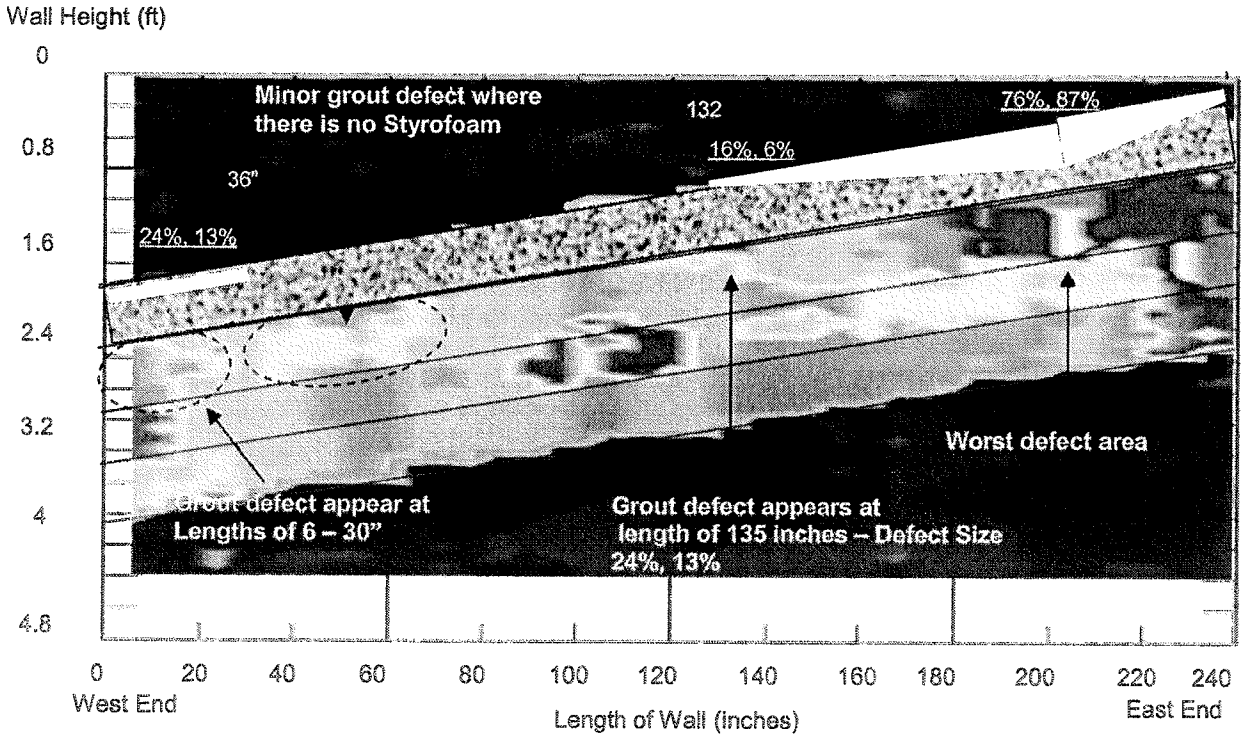

Figure 37 – Comparison of IE results from the Second Duct from Top (South Wall) and the Defect Design

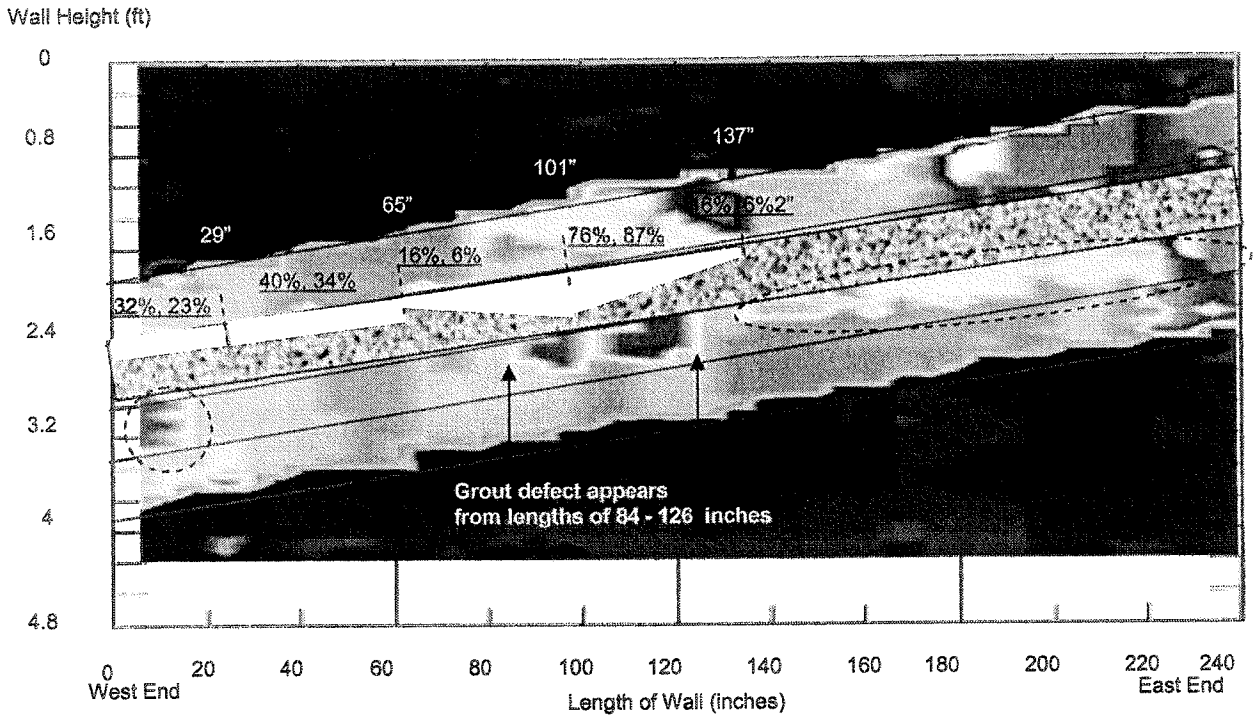

Figure 38 – Comparison of IE results from the Third Duct from Top (South Wall) and the Defect Design

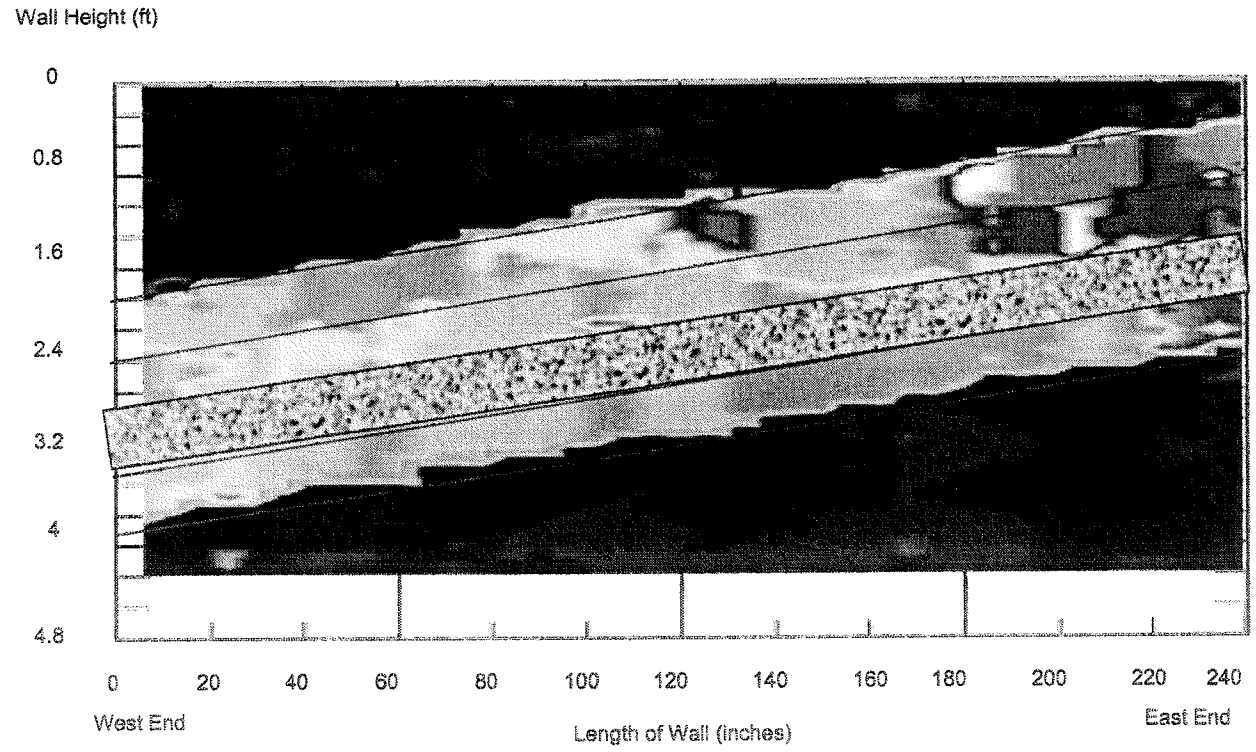

Figure 39 – Comparison of IE results from the Bottom Duct (South Wall) and the Defect Design

Comparisons of the IE results and the defect design of North Wall The results from the North wall are presented in terms of normalized IE thickness which is the ratio of the IE thickness results to the 10 inch nominal wall thickness. The color scale in this case range from blue which represents the nominal thickness of the wall to black which represents 1.6 times the nominal thickness of the wall (see the color scale in Figure 35b).

Top Duct: A comparison of the IES test results from the top duct of the North wall and its defect design (placed above the results from the top duct) is presented in Figure 40. Review of Figure 40 shows that a grout defect appears immediately at the west end of the duct where there is no Styrofoam. However, visual inspection of the girder showed honeycomb void around the duct at the west end. The IE results show grout defect from the west end all the way towards the east end. The grout defect becomes clearly apparent (change to black color) where the size of grout defect is half size duct diameter.

Second Duct from Top: A comparison of the IES test result from the second duct from top of the North wall and its defect design (placed above the results from the second duct from top) is presented in Figure 41. Review of Figure 41 shows no indication of a grout defect where the smallest grout defect was placed (16% perimeter lost or 6% depth lost). The grout defect becomes more apparent at location where grout defect size of 24% perimeter lost or 13% depth lost was placed. In addition, Figure 39 indicates the worst grout defect area (east end) at the location where the biggest Styrofoam defect was placed.

Third Duct from Top: A comparison of the IES test results from the third duct from top of the North wall and its defect design (placed above the results from the third duct from top) is presented in Figure 42. Review of Figure 42 shows that a grout defect appears at a length of 102" from the west end. This location corresponds to a defect size of 20% perimeter lost or 11% depth lost.

Bottom Duct: The comparison of the results from the bottom duct and the design is not included herein. The duct was originally was designed to hold water. However, water leaked out through the loose plug by the time the testing begun. Therefore, the duct was empty during the time of the IE testing and only showed void conditions.

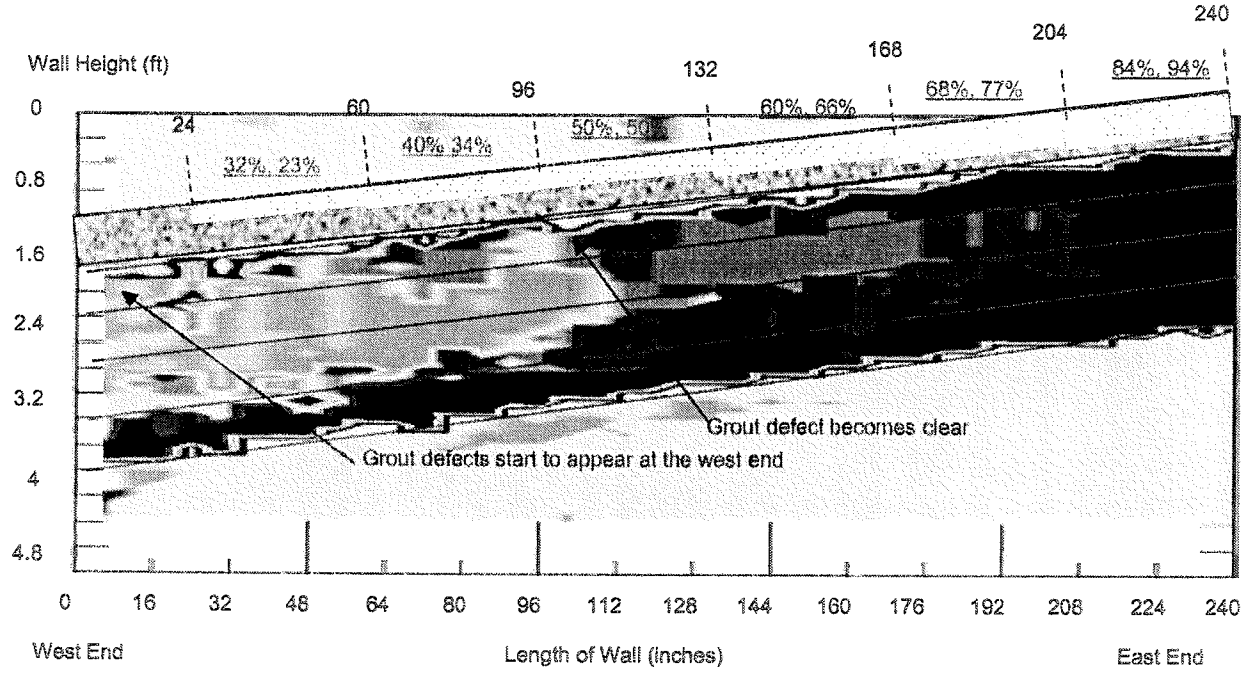

Figure 40 – Comparison of IE results from the Top Duct (North Wall) and the Defect Design and relative normalized to wall thickness color scale below.

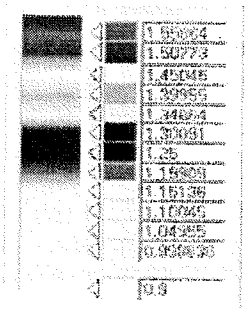

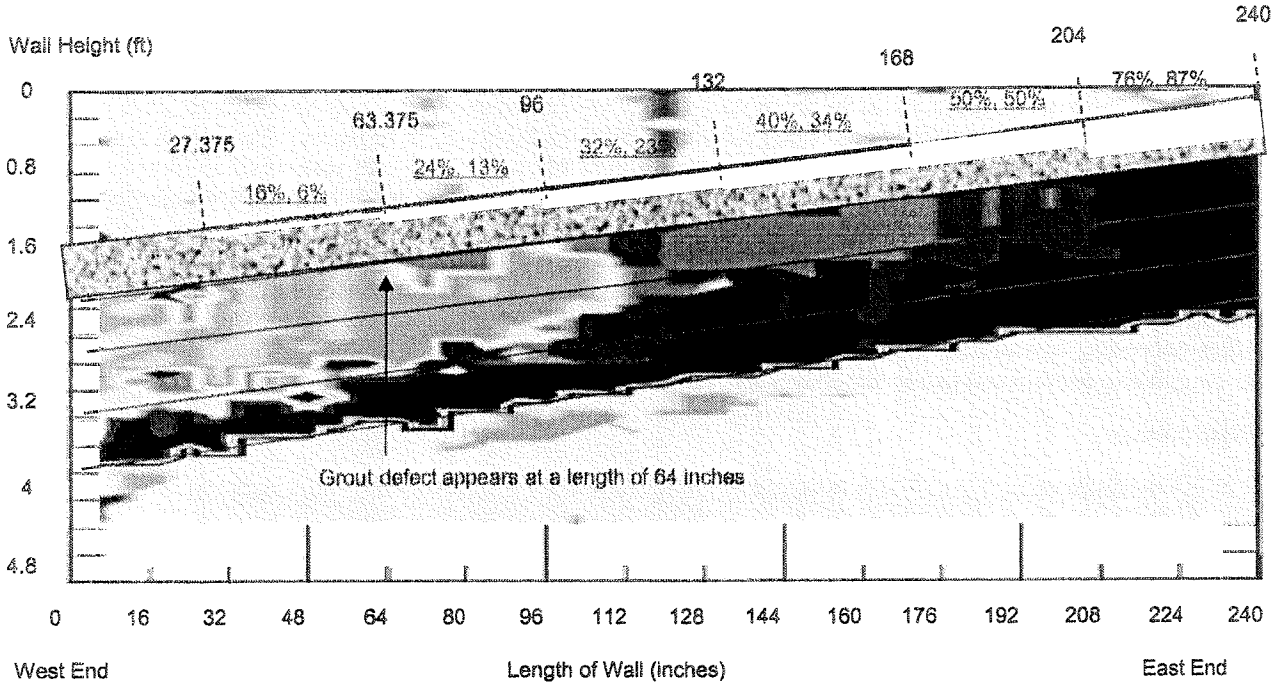

Figure 41– Comparison of IE results from the Second Duct from Top (North Wall) and the Defect Design

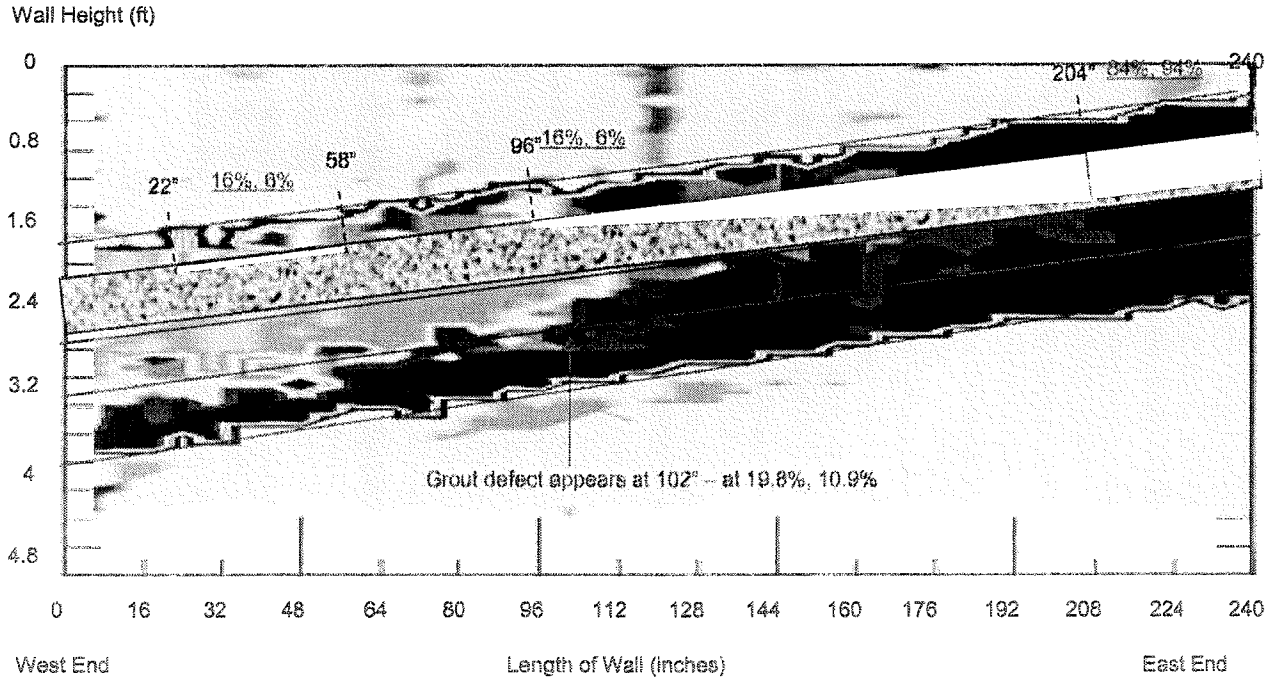

Figure 42– Comparison of IE results from the Third Duct from Top (North Wall) and the Defect Design

6.3.2 Ultrasonic Pulse Echo (UPE) Test Results

The UPE tests were performed only on the South wall. The B scan test result from a wall area with no ducts is presented in Figure 43. Review of Figure 43 shows strong reflections from the back wall at 10 inches. The B scan test result from an area with ducts is presented in Figure 44. Review of Figure 44 shows back wall reflections at 10 inches and duct echoes at approximately 4.5 inches toward the left end. Figure 45 shows a 3D result from the UPE tests on the South wall. The X scale represents the length of the girder. The Y scale shows the height of the girder and the Z scale represents the reflection location inside the girder. In this case, the backwall reflection is approximately 10 inches represented in red color and a stripe of four ducts diagonally in the middle can be identified in blue color (4 inches deep from the test surface). Unfortunately, the UPE tests were unable to detect beyond the ducts. This could be because of possible debonding between the grout and ducts as the UPE tests were performed on the wall approximately 12 months after the grouting process and defect installation was complete.

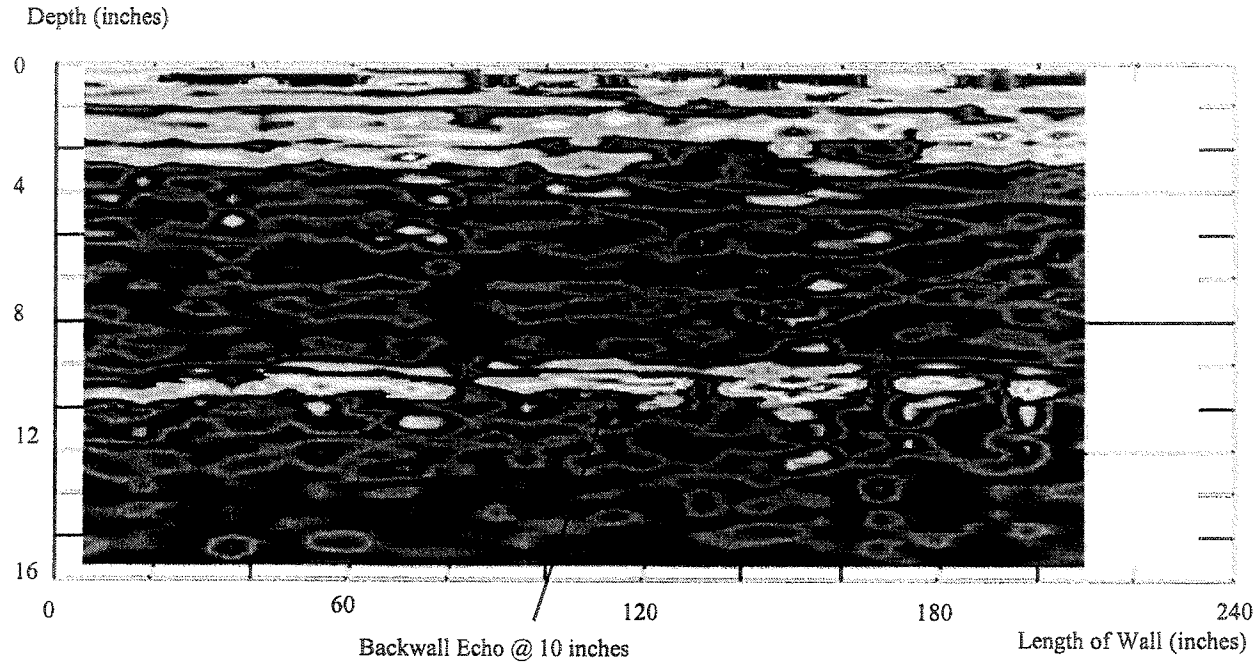

Figure 43 – B Scan Result from UPE tests on the Top of South Wall (no Duct inside) showing Backwall Echo

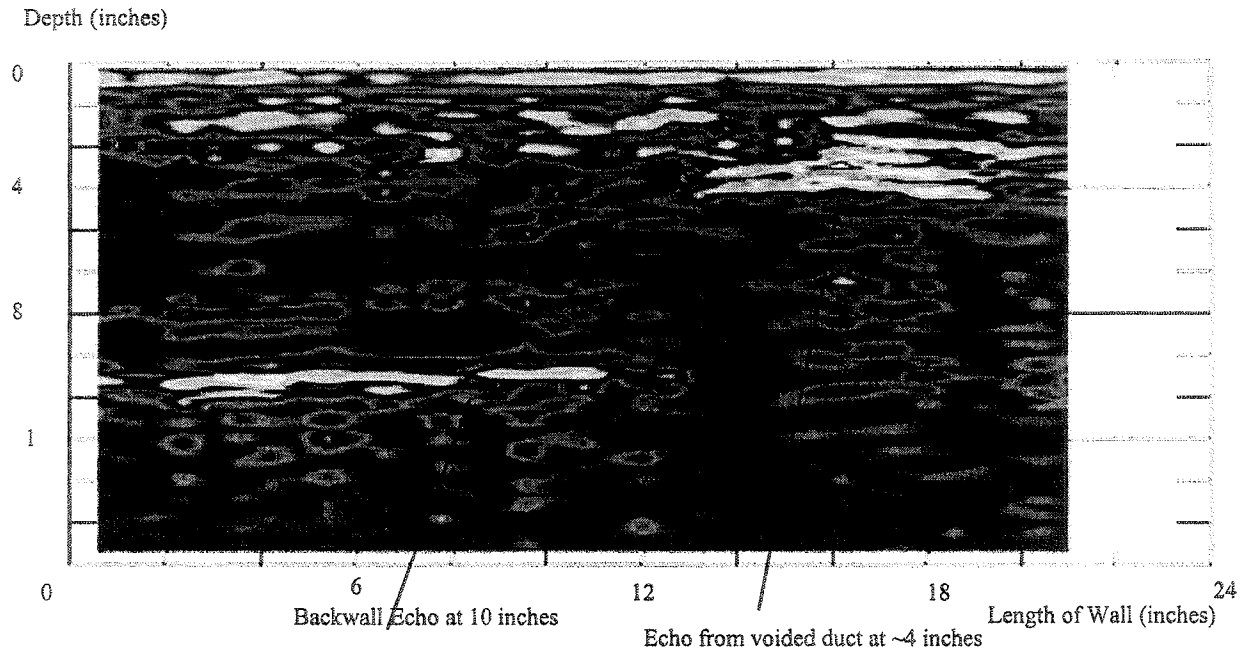

Figure 44 – B Scan Result from UPE tests in the South Wall Area with ducts on the East End

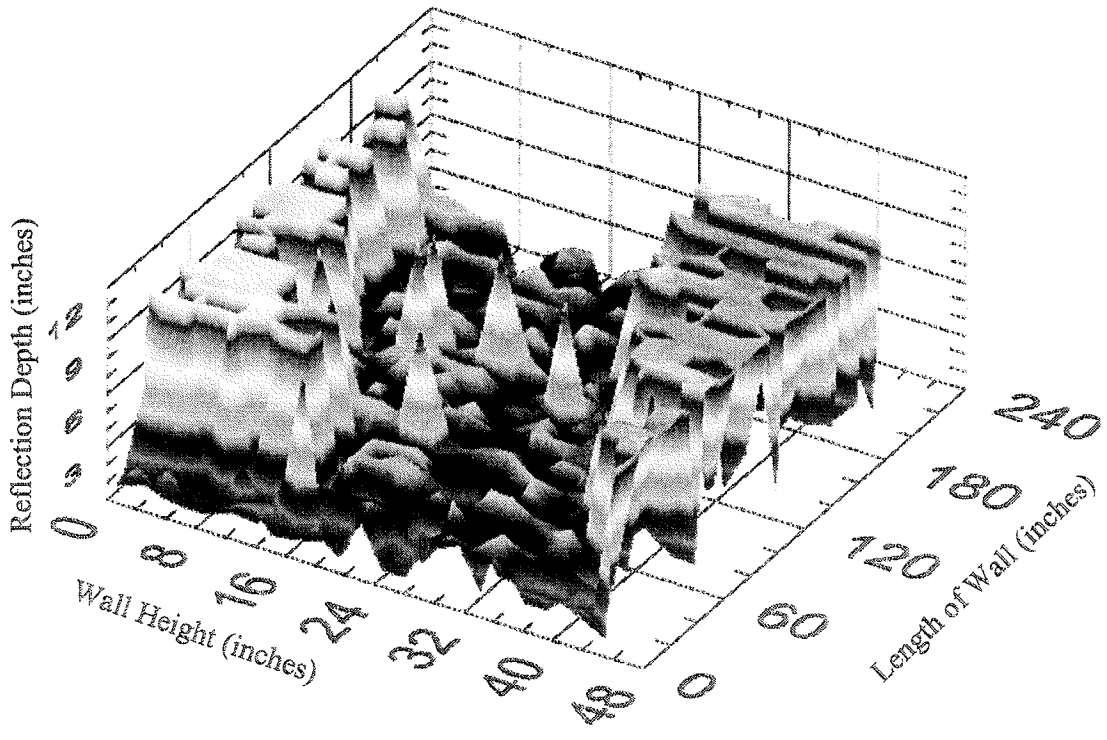

Figure 45 – 3 D Surface Plot of the Reflection from the UPE Tests on the South Wall

7.0 CONCLUSIONS

In summary, the objective of the research was achieved using a rolling Impact Echo Scanner. Very small grout defects were detected in a 4" duct. The results from the sensitivity studies of grout defects as well as other improvements of the Impact Echo Scanning system have resulted in increases in the reliability of the test results for the evaluation of internal grout/void condition of post-tensioned bridge ducts. The scanning capability tremendously reduces the field testing process and provides near continuous test results. A direct impact of the results of the research is to improve quality assurance programs of grout to mitigate tendon corrosion risks for new post-tensioned bridges. The results can also be integrated into bridge maintenance and inspection programs for existing post-tensioned bridges to help prevent partial or catastrophic failures.

The research showed that the current Impact Echo Scanning technology can be used effectively to detect very small grout defects in 4" steel ducts (with 3" concrete cover). Half size and full size voids can be detected with the IE tests in 4.72" and 3.94" ducts. Only full size voids can be detected inside ducts with a diameter of 3.15 inches. However, the limitation of the current technology is that once the concrete cover is 5.5 inches and higher, the IE results become intermittent and unreliable.

The results from this research project can also be used to investigate voids and honeycomb in other concrete structures aside from the post-tensioned bridge ducts. With the scanning ability to expedite the field tests and more reliable results from the combined tests between Impact Echo and Spectral Analysis of Surface Waves tests, this will encourage the use of non-destructive evaluation (NDE) for internal condition assessment of a wide variety of structures/infrastructure. Eventually, it will lead to improved integrity and safety of structures and infrastructure. Parts of the results from the research are already made available to the international research community through publication of results publications at leading conferences and journals including Materials Evaluation (the official journal of American Society for Nondestructive Testing) (6).

Future research should focus on new type of sensor technology such as air-coupled sensors. A comparative study between the dry mounted rolling transducer and the air-coupled sensors will be informative. In addition, more detailed research in the sensitivity study of grout defects in smaller diameter ducts should be encouraged.

To date, Impact Echo Scanning has been used by the authors in the testing of about 10 bridges across the US and one bridge in England on a consulting basis. Also, Impact Echo Scanner systems have been sold to several universities/research institutes in China and Saudi Arabia in the past year through Olson Instruments, Inc. Based on the successful research results reported herein, the PI and Co-PI plan to apply for Phase II funding to further advance technologies for stress-wave scanning to evaluate grout/void conditions in post-tensioning ducts of bridges.

8.0 INVESTIGATOR PROFILES

Key investigators for the research project include Dr. Yajai Tinkey as a Principal Investigator and Mr. Larry D. Olson as a CO-PI. Dr. Tinkey has a computer engineering and structural engineering background. She has intensive experience with non-destructive evaluation methods applied to structures and infrastructure. These NDE methods include both Impact Echo and Ultrasonic tests. Dr. Tinkey has developed a number of non-destructive testing analysis software programs available for in-house and commercial uses. Prior this research project, she was heavily involved in a feasibility research project (Nondestructive Evaluation Research internal grout condition inside steel and Plastic Post-Tensioned Ducts) which was directed by Dr. Larry Muszynski of University of Florida (funded by Florida Department of Transportation).

Mr. Larry Olson is President and Principal Engineer of Olson Engineering, Inc. Mr. Olson has a background in geotechnical, materials and pavement engineering and has over 25 years of non-destructive evaluation and structural condition assessment experience. Mr. Olson previously served as a PI for a number of research projects funded by different government organizations. He developed shear and compressional wave sensors and sources for an offshore bottom-hole seismic device in his Master's research and continues to be actively involved in development of sensor/source hardware systems. He is the primary US patent holder and inventor of the Impact Echo Scanner technology.

Dr. Yajai Tinkey (Yajai@olsonengineering.com) and Mr. Larry Olson (ldolson@olsonengineering.com) can be contacted at the Olson Engineering, Inc. main office located at 12401 W. 49th Ave, Wheat Ridge, Colorado (phone: 303-423-1212).

9.0 REFERENCES

[1] Concrete Society Technical Report No. 47, "Durable Bonded Post-Tensioned Concrete Bridges", Concrete Society, 1996

[2] Woodward, R.J. and Williams, F.W., "Collapse of the Ynys-y-Gwas Bridge, West Glamorgan," *Proceeding of The Institution of Civil Engineers*, Part 1, Vol. 84, August 1988, pp. 635-669.

[3] Florida Department of Transportation (FDOT) Central Structures Office, "Test and Assessment of NDT Methods for Post Tensioning Systems in Segmental Balanced Cantilever Concrete Bridges, Report, February 15, 2003.

[4] J. S. West, C. J. Larosche, B. D. Koester, J. E. Breen, and M. E. Kreger, "State-of-the-Art Report about Durability of Post-tensioned Bridge Substructures", Research Report 1405-1, *Research Project 0-1405,* Texas Department of Transportation, October 1999.

[5] D. Sack and L.D. Olson, "Impact Echo Scanning of Concrete Slabs and Pipes", International Conference on Advances on Concrete Technology, Las Vegas, NV, June 1995

[6] Y. Tinkey, L.D. Olson, H. Wiggenhauser , "Impact Echo Scanning for Discontinuity Detection and Imaging in Posttensioned Concrete Bridges and Other Structures", Materials Evaluation, January 2005, pp 64-69.